Fundamental Bands of $^{32}S^{16}O_2$

K. Fox
G.D.T. Tejwani
R.J. Corice, Jr.

September 1972

Earth Resources
and
Astrophysics Laboratory
Department of
Physics and Astronomy
THE UNIVERSITY OF TENNESSEE
Knoxville, Tennessee

Addenda and Errata

to

UTPA-ERAL-01

Page	Line	Addenda or Errata
30	footnote f, add	These values have been corrected for hot band contributions in Ref. 31.
31	20 21 - 22	found several relatively for example, with observed positions at 543.60, 1132.03
	22	(see Tables III - V)
	24	for some other lines
33	Ref. 24	J. Chem. Phys. 58, 265 (1973).
34	Ref. 31	Chem. Phys. Letters, to be published, 1973.
	Ref. 34	W. W. Kellogg
	Ref. 36	J. Chem. Phys. 57, 4676 (1972).

FUNDAMENTAL BANDS OF $^{32}S^{16}O_2$

K. Fox

G. D. T. Tejwani

R. J. Corice, Jr.

Research Report No. UTPA-ERAL-01

September 1972

Earth Resources and Astrophysics Laboratory

Department of Physics and Astronomy

The University of Tennessee

Knoxville, Tennessee 37916

This work was supported in part by Multidisciplinary Research Grant NGL-43-001-021 from the National Aeronautics and Space Administration. A preliminary report of part of this work was presented at the Symposium on Molecular Structure and Spectroscopy, The Ohio State University, Columbus, 12-16 June 1972, Abstract W2.

CONTENTS

ABSTRACT

The infrared-active vibration-rotation fundamentals of sulfur dioxide have been measured with moderately high spectral resolution. Quantum number assignments have been made for spectral lines from $J = 0$ to 57, by comparison with theoretically computed spectra which include the effects of centrifugal distortion. The following values for the band centers have been determined: $\nu_1^\circ = 1151.65 \pm 0.10\ cm^{-1}$, $\nu_2^\circ = 517.75 \pm 0.10\ cm^{-1}$, and $\nu_3^\circ = 1362.00 \pm 0.10\ cm^{-1}$. Intensities of the observed lines have also been computed. Dipole moment derivatives have been obtained.

I. INTRODUCTION

Nearly twenty years have passed since the important systematic observation of 17 infrared-active vibration-rotation bands of sulfur dioxide by Shelton, Nielsen, and Fletcher.[1] In that work on $^{32}S^{16}O_2$, unfavorable energy and detector conditions in several spectral regions necessitated the use of slits ranging from 0.30 to 2.00 cm^{-1}. Consequently, it was not possible to resolve individual transitions, and only sub-branches were assigned.

More recently, high-resolution microwave and far-infrared spectra of SO_2 arising from pure rotational transitions in the ground and excited states have been obtained.[2-7] From analyses of these spectra, accurate values of rotational and centrifugal distortion constants are available. Hinkley et al.[8] have now observed some individual transitions of the ν_1 vibration-rotation bands of SO_2 using tunable semiconductor lasers with very high resolution.[9] Prior to our knowledge of this most recent work,[8,9] we undertook moderately high-resolution studies of all three infrared-active fundamentals of $^{32}S^{16}O_2$ in order to assign as many individual vibration-rotation transitions as possible.

The experimental details for our absorption spectra are discussed in the next Section. In Section III, asymmetric rotor theory is reviewed briefly. Then we present our results in the form of measured spectra, and tabulated experimental and theoretical positions for more than twelve hundred lines. In the last Section, we discuss future studies in which certain experimental and theoretical advances may be expected. Finally, we consider the potential application of our results to laser science and to air pollution problems.

II. EXPERIMENTAL DETAILS

The anhydrous grade $^{32}S^{16}O_2$ gas sample was obtained from Matheson Gas Products. The stated purity of the sample was 99.98% by weight; with 50, 10, and 30 p.p.m. maxima of H_2O, H_2SO_4, and non-volatiles, resp. A Perkin-Elmer Model 225 Grating Infrared Spectrophotometer, equipped with an f/5 fore monochromator for pre-dispersion of the radiation, was

used to record the spectra. A 150 lines/mm grating was employed in the first order for the 1100 to 1400 cm^{-1} region, and a 30 lines/mm grating in the second order for the 475 to 600 cm^{-1} region. A servo-controlled slit program was utilized to provide constant energy to the thermopile detector. A filtered Sola transformer served as a power supply which minimized external electrical noise and provided a constant voltage to the spectrophotometer.

Before each run, the alignment of the Littrow mount in the fore monochromator, and the position of the thermopile relative to the emerging radiation source were precisely adjusted to maximize signal strength. All scans were recorded on a Model 225 Auxiliary Recorder at a speed of 0.5 cm^{-1}/min at suitable scale expansions. A minimum of five runs was taken for each vibration-rotation band. The best two runs with respect to reproducibility, resolution, and noise level were selected for the theoretical analysis of each band.

Two 10-cm absorption cells, one with NaCl and the other with KBr windows, were used. The cells were placed in the sample compartment for one hour prior to each run in order to stabilize (at approximately 315°K) the temperature increase caused by heating from the Globar radiation source.

The details of our experimental conditions are summarized in Table I. Several runs of ν_2 were also made using cells with KRS-5 windows. However, it was found that substantially higher energy was available with the KBr windows due to their lower refractive index; hence, narrower slits could be used. For calibration purposes, spectra[10-11] with resolution comparable to that achieved in the present work were chosen. In spite of the larger slit width and lower dispersion in our measurements of ν_2, the absolute accuracy in its line positions is the same as that for ν_1 and ν_3 because of a better intercomparison with the calibration lines.[11]

TABLE I

EXPERIMENTAL CONDITIONS

	ν_1	ν_2	ν_3
Pressure (torr)	30	40	1
Temperature (°K)	315 ± 5	315 ± 5	315 ± 5
Cell length (cm)	10	10	10
Window material	NaCl	KBr	NaCl
Slit width (cm^{-1})[a]	0.16 ± 0.02	0.32 ± 0.09	0.17 ± 0.02
Dispersion (cm/cm^{-1})[b]	2.5	1	2.5
Calibration band	ν_2 of NH_3[c]	ν_5 of C_2D_2[d]	ν_4 of CH_4[c]
Relative accuracy (cm^{-1})	± 0.05	± 0.05	± 0.05
Absolute accuracy (cm^{-1})	± 0.10	± 0.10	± 0.10
Grating (lines/mm)	150	30	150
Grating (order)	first	second	first

[a] Obtained directly from instrumental readings; errors represent maximum range of values.

[b] Determined from comparisons of SO_2 and calibration lines recorded at identical instrumental settings; errors are less than 1%.

[c] From Ref. 10.

[d] From Ref. 11.

III. THEORETICAL ANALYSIS

The sulfur dioxide molecule is an asymmetric rotor with C_{2v} symmetry,[12] whose bond length and bond angle are 1.4308 Å and 119°20', resp.[7] As the theory of asymmetric top spectra is well known,[12,13] only a brief review pertinent to present work will be given. From Kivelson and Wilson's[14] theory for first-order centrifugal distortion, with the inclusion of second-order terms[15] up to $\langle P_z^4 \rangle$, the energy expression is

$$E = E_r - [D_J+2R_6]J^2(J+1)^2 - [D_{JK}-4R_6]J(J+1)\langle P_z^2\rangle$$

$$- [D_K+2R_6]\langle P_z^4\rangle + 2\sigma\delta_J[\langle P_z^2\rangle - W]J(J+1)$$

$$+ 4R_5\sigma[\langle P_z^2\rangle W - \langle P_z^4\rangle] + 4R_6\sigma^2[\langle P_z^4\rangle - 2\langle P_z^2\rangle W + W^2]$$

$$+ H_{JK}J^2(J+1)^2\langle P_z^2\rangle + H_{KJ}J(J+1)\langle P_z^4\rangle, \qquad (1)$$

where

$$E_r = \frac{1}{2}(B+C)J(J+1) + [A - \frac{1}{2}(B+C)]W(b_p), \qquad (2)$$

$$\sigma = -1/b_p = (2A - B - C)/(B-C), \qquad (3)$$

and A, B, and C are the rotational constants in order of decreasing magnitude. E_r is the rigid rotor energy and $W \equiv W(b_p)$ is the Wang reduced energy. J is the quantum number corresponding to the total angular momentum operator with molecule-fixed z-component P_z. General formulas for the expectation values $\langle P_z^2\rangle$ and $\langle P_z^4\rangle$ have been given in Ref. 14. The D's, R's, and σ_J are linear combinations of the τ's, coefficients of centrifugal distortion.[14]

The absolute intensity of an absorption line corresponding to a transition between initial and final states with quantum numbers n" and n', resp., is[16]

$$I_{n"n'} = \frac{8\pi^3 N g_{n"} \nu[1-\exp(-h\nu/kT)]\exp(-E_{n"}/kT)}{3hcp \sum_{n"} g_{n"} \exp(-E_{n"}/kT)} \times |\mu_{n"n'}|^2, \qquad (4)$$

where N is the number of molecules per cm^3, $\nu \equiv (E_{n'} - E_{n"})/h$ is the central frequency of the line, and $g_{n"}$ is the statistical weight factor. The quantity $\mu_{n"n'}$ is the expectation value of the transition dipole moment, p and T are the gas pressure and temperature, resp., and k, h, and c are universal constants. Eq. (4) can be simplified by collecting into a single constant C all quantities which are essentially unchanged for all the lines of a particular vibration-rotation band. Also, expressing $|\mu_{n"n'}|^2$ in terms of $S^g_{R"R'}$ (the square of the direction cosine matrix element along the molecule-fixed g axis) and dipole-moment derivatives,[17] we obtain for the case of a rigid rotor

$$I^{\circ}_{n''n'} = Cg_{n''}\nu_i[1-\exp(-h\nu_i/kT)][\exp(-E_{R''}/kT)\left(\frac{\hbar}{4\pi c\nu^{\circ}_i}\right)\sum_g S^g_{R''R'}\left(\frac{\partial\mu_g}{\partial Q_i}\right)^2, \quad (5)$$

where R represents the rotational quantum numbers, and Q_i is the normal coordinate for the fundamental vibration ν_i. The band center is denoted by ν°_i.

For a given fundamental vibration, Eq.(5) reduces further to

$$I^{\circ}_{n''n'} = C'g_{n''}\left(\frac{\nu_i}{\nu^{\circ}_i}\right)[1-\exp(-h\nu_i/kT)][\exp(-E_{R''}/kT)\sum_g S^g_{R''R'}, \quad (6)$$

where

$$C' = \frac{\pi N}{3c^2p\sum_{n''} g_{n''}\exp(-E_{n''}/kT)}\left[\left(\frac{\partial\mu_a}{\partial Q_i}\right)^2 \text{ or } \left(\frac{\partial\mu_b}{\partial Q_i}\right)^2\right]. \quad (7)$$

The factorization of Eq.(5) into Eqs.(6) and (7) is a consequence of the fact that the fundamental bands of planar asymmetric rotors such as SO_2 are of only two types. These are denoted by A (as in ν_3) or B (as in ν_1 and ν_2) for which the dipole-moment derivative is along the axis of least (a-axis) or intermediate (b-axis) moment of inertia. Thus

$$\sum_g\left(\frac{\partial\mu_g}{\partial Q_i}\right)^2 = \left(\frac{\partial\mu_a}{\partial Q_i}\right)^2 \text{ or } \left(\frac{\partial\mu_b}{\partial Q_i}\right)^2. \quad (8)$$

For computing line intensities $I^{\circ}_{n''n'}/C'$ and line positions $(E_{n'}-E_{n''})/h$, we have used the computer program originally written by Pierce and modified by Eggers.[18] This program is very compact and fast.[19] In it, the wavenumber range of the entire band is divided into a large number of intervals, each of which may be taken as approximately half a resolution element. The intensity of each transition is assigned to the appropriate interval. When these assignments are completed, the intensity in each interval is distributed over adjacent intervals according to a Gaussian function which takes into account the finite width of the absorption lines. We have used, instead, a triangular distribution function with base equal to twice our experimental slit width. We found that this approach gave the best

TABLE II

ROTATIONAL AND CENTRIFUGAL DISTORTION CONSTANTS FOR $^{32}S^{16}O_2$

Ground State[a]		Excited States[c]	
Constant	Value (in cm^{-1})	Constant	Value (in cm^{-1})
A	2.0273555 ± 0.0000006		ν_1
B	0.3441702 ± 0.0000002		
C	0.2935302 ± 0.0000001	A	2.0284336
τ_{zzzz}	$(-3.3095 \pm 0.0010) \times 10^{-4}$	B	0.3425071
τ_{xxzz}	$(+0.1439 \pm 0.0002) \times 10^{-4}$	C	0.2921169
τ_{xzxz}	$(-0.01775 \pm 0.00018) \times 10^{-4}$		
τ_{xxxx}	$(-0.01331 \pm 0.00003) \times 10^{-4}$		ν_2
H_{KJ}	$(-0.0311 \pm 0.0128) \times 10^{-8}$		
H_{JK}	$(-0.0111 \pm 0.0029) \times 10^{-8}$	A	2.0665828
τ_{yyyy}	-0.004108×10^{-4}	B	0.3442469
τ_{yyxx}	-0.006665×10^{-4}	C	0.2930009
τ_{yyzz}	$+0.03529 \times 10^{-4}$		
D_J	$+0.0020495 \times 10^{-4}$		ν_3
D_K	$+0.865348 \times 10^{-4}$		
D_{JK}	$-0.0400224 \times 10^{-4}$	A	2.0066777
R_5	$+0.0048567 \times 10^{-4}$	B	0.3430118
R_6	$-0.0063875 \times 10^{-6}$	C	0.2924378
δ_J	$+0.00575125 \times 10^{-5}$		
σ	67.47651[b]		

[a] The first nine values are taken from Ref. 4, the next three are calculated from Eqs. (9-11) of Ref. 15, and the remaining seven are calculated from relations (36) of Ref. 14.

[b] Dimensionless, see Eq. (3).

[c] The values for ν_1 are taken from Ref. 6, and those for ν_2 and ν_3 are taken from Ref. 2.

agreement between the calculated theoretical spectrum and the overall detailed appearance of our experimental spectrum.

Rotational and centrifugal distortion constants, in the ground and excited vibrational states of SO_2, used in the computer program have been taken from far-infrared[4] and microwave[2,6] spectra. These values and the remaining derived values, calculated from the relations in Refs. 14 and 15, are given in Table II. The computer program takes into account the fact that in the ground state of SO_2 only symmetric levels occur because of C_{2v} symmetry and zero spin of the ^{16}O nuclei. The initial values for the three band centers were taken from the work of Shelton et al.[1] These values were later adjusted so that the experimental and theoretical spectra would match.

The dipole moment derivatives for the fundamentals were calculated in the following way. Equation (6) was summed over all transitions having $J \leq 60$. Previously measured experimental band intensities,[20-23] and a projected value,[8] were taken for $\sum_{n''n'} I^{\circ}_{n''n'}$. Our calculated line intensities were used for the sum on the right hand side of Eq.(6), so that C' was determined. The sum over n'' in Eq.(7) could be factored, to a good approximation, into a vibrational and a rotational partition function which were readily evaluated from Eqs.(V,17) and (V,29), resp., of Ref. 12. Finally, from the value of C' obtained using Eq.(6), the dipole moment derivatives were deduced from Eq.(7). As the derivatives occur squared in Eq.(7), only their absolute values could be determined by this method.

IV. RESULTS

The results of our experimental and theoretical studies of the fundamental infrared bands of $^{32}S^{16}O_2$ are summarized in Figs. 1-3 and Tables III-VI. A representative portion of these results have also been presented in Ref. 24. The experimental conditions were given in Table I. Spectral resolution in the 1100-1400 cm^{-1} region for ν_1 and ν_3 was typically about 0.12 cm^{-1}, with isolated instances of 0.10 cm^{-1} or better. In the 475-600 cm^{-1} region for ν_2, resolution was characteristically 0.25 cm^{-1}, and occasionally 0.20 cm^{-1} or better. In the Figures, the upper tracings are the measured experimental spectra, with percent absorption shown in the right-hand vertical scales. It should be noted that both the measured spectra and the right-hand scales are displaced upward by the same amount,

so that 0% absorption denotes the experimental base line.

Our calculated theoretical spectra are also represented in Figs. 1-3. These spectra are the lower tracings, with relative intensity on the left-hand vertical scales. The intensity plotted in the Figures is a normalized distribution of line intensities. This distribution into small intervals was discussed in Sec. III. The normalization, on a linear scale, is made with respect to that distribution of intensities (arbitrarily assigned the value 100 for ν_1 and ν_3, and 90 for ν_2) which is the maximum for all the intervals in a given band. As can be seen in the Figures, there is good agreement between the theoretical and experimental spectra.

In Tables III-V, the observed and computed spectral line positions are compared. Only the stronger theoretical transitions corresponding to each experimental line peak have been listed in these Tables. (Where there is a blank space in the column of experimental line positions, the adjacent theoretical line position corresponds to the previously tabulated experimental line.) With very few minor exceptions, 97% of the tabulated computed lines fall within ± 0.05 cm^{-1} of the observed lines. Initial- and final-state quantum number assignments, as well as theoretical line intensities $I^{\circ}_{n''n'}/C'$ defined by Eq.(6), are given for the computed lines in Tables III-V. The quantum numbers K_{-1} and K_1 are associated with the projection of the total angular momentum (having quantum number J) on the symmetry axis in, resp., the prolate and oblate symmetric top limiting cases.[12,13]

Experimental and theoretical results for ν_1 in the spectral range from 1112.5 to 1200.0cm^{-1} are represented in Fig. 1 and Table III. The selection rules[25] are $\Delta J = 0, \pm 1$; $J = 0 \nleftrightarrow J = 0$; and ΔK_{-1} and $\Delta K_1 = \pm 1, \pm 3, \ldots$. Approximately 450 observed lines have now been assigned. The band center for ν_1 has been determined in the present work to be 1151.65 $\pm$ 0.10 cm^{-1}. Earlier infrared observations yielded the values 1152 (Ref. 26), 1151.38 (Refs. 27 and 1), 1152 $\pm$ 1 (Ref. 28), and 1151.2 $\pm$ 0.2 cm^{-1} (Ref. 29). Most recently, Hinkley *et al.*,[8] using very high resolution (line width less than 10^{-5} cm^{-1}) techniques, have found a value of 1151.71 $\pm$ 0.01 cm^{-1} in excellent agreement with our result, to within our experimental error. We have also compared our calculated line positions, taking into account the 0.06 cm^{-1} difference in band centers, to the several rather isolated

TABLE III

COMPARISON OF EXPERIMENTAL AND THEORETICAL SPECTRAL LINE POSITIONS, WITH QUANTUM NUMBER ASSIGNMENTS, FOR THE ν_1 BAND OF $^{32}S^{16}O_2$ CENTERED AT 1151.65±0.10 cm^{-1}. LINE INTENSITIES [SEE SEC.III, ESPECIALLY EQ. (6)] ARE COMPUTED AT 300°K.

Line Position (in cm^{-1})		Quantum Numbers							Line Position (in cm^{-1})		Quantum Numbers						
Exptl.	Theor.	J'	K'_{-1}	K'_1	J"	K''_{-1}	K''_1	$\frac{I^\circ_{n''n'}}{C'}$	Exptl.	Theor.	J'	K'_{-1}	K'_1	J"	K''_{-1}	K''_1	$\frac{I^\circ_{n''n'}}{C'}$
1112.68	1112.70	29	5	25	30	6	24	1.5189		1119.77	9	7	3	10	8	2	3.6800
1112.77	1112.80	24	6	18	25	7	19	2.1767	1120.06	1120.04	24	4	20	25	5	21	2.1291
1112.96	1112.94	19	7	13	20	8	12	2.7233	1120.34	1120.35	18	5	13	19	6	14	2.9815
1113.07	1113.07	14	8	6	15	9	7	3.1098	1120.44	1120.41	13	6	8	14	7	7	3.4418
1113.17	1113.17	9	9	1	10	10	0	3.3979		1120.44	8	7	1	9	8	2	3.7582
1113.48	1113.50	23	6	18	24	7	17	2.3113	1120.59	1120.56	25	3	23	26	4	22	1.3955
1113.66	1113.63	18	7	11	19	8	12	2.8427	1120.77	1120.73	46	0	46	47	1	47	1.6644
1113.79	1113.76	13	8	6	14	9	5	3.2075	1120.99	1120.94	38	8	30	38	9	29	1.0263
1113.87	1113.87	41	10	32	41	11	31	0.5309		1121.04	17	5	13	18	6	12	3.1023
1114.06	1114.11	27	5	23	28	6	22	1.7850	1121.09	1121.09	12	6	6	13	7	7	3.5155
1114.17	1114.20	22	6	16	23	7	17	2.4453		1121.10	7	7	1	8	8	0	3.8452
1114.28	1114.33	17	7	11	18	8	10	2.9578	1121.21	1121.23	22	4	18	23	5	19	2.4065
1114.40	1114.44	12	8	4	13	9	5	3.3020	1121.38	1121.37	33	8	26	33	9	25	1.5005
1114.58	1114.61	34	10	24	34	11	23	0.9517	1121.55	1121.51	44	1	43	45	2	44	1.5687
1114.77	1114.71	33	10	24	33	11	23	1.0171	1121.75	1121.72	16	5	11	17	6	12	3.1934
1114.85	1114.89	26	5	21	27	6	22	1.9247		1121.76	11	6	6	12	7	5	3.5817
	1114.90	21	6	16	22	7	15	2.5771	1121.94	1121.95	38	3	35	39	4	36	1.1678
1114.98	1115.02	16	7	9	17	8	10	3.0674	1122.11	1122.08	24	8	16	24	9	15	2.2396
1115.08	1115.11	11	8	4	12	9	3	3.3934		1122.15	23	8	16	23	9	15	2.2793
1115.28	1115.25	27	10	18	27	11	17	1.3696	1122.59	1122.56	16	8	8	16	9	7	2.0485
1115.50	1115.51	25	5	21	26	6	20	2.0607		1122.61	15	8	8	15	9	7	1.9208
1115.57	1115.59	20	6	14	21	7	15	2.7059	1122.83	1122.86	43	1	43	44	0	44	2.3009
1115.69	1115.71	15	7	9	16	8	8	3.1714	1123.08	1123.09	14	5	9	15	6	10	3.3624
1115.82	1115.79	10	8	2	11	9	3	3.4844		1123.10	9	6	4	10	7	3	3.6957
1115.91	1115.89	18	10	8	18	11	7	1.3601	1123.53	1123.48	40	2	38	41	3	39	1.6539
	1115.95	17	10	8	17	11	7	1.2821		1123.57	42	0	42	43	1	43	2.5460
1116.27	1116.24	24	5	19	25	6	20	2.2012	1123.80	1123.77	13	5	9	14	6	8	3.4379
	1116.29	19	6	14	20	7	13	2.8305		1123.77	8	6	2	9	7	3	3.7491
1116.47	1116.46	9	8	2	10	9	1	3.5768	1124.13	1124.13	44	7	37	44	8	36	0.6816
1116.97	1116.98	18	6	12	19	7	13	2.9500	1124.31	1124.27	41	1	41	42	0	42	2.8072
1117.05	1117.07	13	7	7	14	8	6	3.3608		1124.32	40	1	39	41	2	40	2.3157
1117.16	1117.13	8	8	0	9	9	1	3.6753	1124.41	1124.44	7	6	2	8	7	1	3.8059
1117.59	1117.61	22	5	17	23	6	18	2.4758		1124.44	12	5	7	13	6	8	3.4980
1117.71	1117.67	17	6	12	18	7	11	3.0635	1124.57	1124.61	39	3	37	40	2	38	1.7928
	1117.75	12	7	5	13	8	6	3.4463	1124.76	1124.77	38	2	36	39	3	37	1.9297
1118.01	1118.00	28	4	24	29	5	25	1.5874	1124.98	1124.97	40	0	40	41	1	41	3.0845
1118.12	1118.11	32	9	23	32	10	22	1.3260	1125.14	1125.10	6	6	0	7	7	1	3.8752
1118.34	1118.31	21	5	17	22	6	16	2.6091		1125.14	11	5	7	12	6	6	3.5581
	1118.36	16	6	10	17	7	11	3.1700	1125.36	1125.35	25	7	19	25	8	18	2.6148
1118.48	1118.43	11	7	5	12	8	4	3.5272	1125.46	1125.42	24	7	17	24	8	16	2.6826
1118.65	1118.62	26	9	17	26	10	16	1.7482		1125.48	23	7	17	23	8	16	2.7364
	1118.70	25	9	17	25	10	16	1.7966	1125.60	1125.55	22	7	15	22	8	14	2.7744
1119.02	1118.98	20	5	15	21	6	16	2.7392		1125.61	21	7	15	21	8	14	2.7944
	1119.05	15	6	10	16	7	9	3.2690	1125.69	1125.67	39	1	39	40	0	40	3.3775
1119.30	1119.27	16	9	7	16	10	6	1.5863	1125.83	1125.79	10	5	5	11	6	6	3.5865
	1119.32	15	9	7	15	10	6	1.4597		1125.88	16	7	9	16	8	8	2.5607
1119.38	1119.37	14	9	5	14	10	4	1.3056	1126.06	1126.02	13	7	7	13	8	6	2.0840
	1119.41	13	9	5	13	10	4	1.1210		1126.06	12	7	5	12	8	4	1.8561
1119.62	1119.66	19	5	15	20	6	14	2.8635	1126.14	1126.13	19	3	17	20	4	16	2.4674
1119.73	1119.73	14	6	8	15	7	9	3.3595	1126.37	1126.37	38	0	38	39	1	39	3.6848

TABLE III (Continued)

Line Position (in cm^{-1})		Quantum Numbers							Line Positions (in cm^{-1})		Quantum Numbers						
Exptl.	Theor.	J'	K'_{-1}	K'_1	J"	K''_{-1}	K''_1	$\frac{I^\circ_{n''n'}}{C'}$	Exptl.	Theor.	J'	K'_{-1}	K'_1	J"	K''_{-1}	K''_1	$\frac{I^\circ_{n''n'}}{C'}$
1126.45	1126.46	9	5	5	10	6	4	3.6173	1132.37	1132.32	28	1	27	29	2	28	4.9822
1126.60	1126.61	44	1	43	44	2	42	0.5291		1132.37	21	5	17	21	6	16	3.8563
1126.72	1126.74	20	3	17	21	4	18	2.5034		1132.42	20	5	15	20	6	14	3.8760
1127.08	1127.06	37	1	37	38	0	38	4.0059	1132.57	1132.55	17	5	13	17	6	12	3.7769
	1127.12	8	5	3	9	6	4	3.6422		1132.60	16	5	11	16	6	10	3.6857
1127.71	1127.75	36	0	36	37	1	37	4.3388	1132.67	1132.64	15	5	11	15	6	10	3.5412
1128.15	1128.14	32	2	30	33	3	31	2.6734		1132.68	14	5	9	14	6	8	3.4059
	1128.15	35	6	30	35	7	29	1.8199		1132.71	13	5	9	13	6	8	3.2143
1128.25	1128.27	33	6	28	33	7	27	2.0920	1132.91	1132.87	8	5	3	8	6	2	1.7618
	1128.29	34	6	28	34	7	27	1.9569		1132.88	18	2	16	19	3	17	2.8849
1128.41	1128.37	32	6	26	32	7	25	2.2303		1132.89	7	5	3	7	6	2	1.1855
	1128.39	31	6	26	31	7	25	2.3657		1132.96	29	3	27	30	2	28	2.8422
	1128.44	35	1	35	36	0	36	4.6825	1133.09	1133.13	4	4	0	5	5	1	3.4208
	1128.45	6	5	1	7	6	2	3.6888	1133.19	1133.17	28	0	28	29	1	29	7.1542
1128.51	1128.49	11	4	8	12	5	7	3.4145		1133.21	9	3	7	10	4	6	3.1590
1128.67	1128.63	27	6	22	27	7	21	2.8713	1133.34	1133.31	13	2	12	14	3	11	2.4385
	1128.69	26	6	20	26	7	19	2.9794	1133.44	1133.48	27	2	26	28	1	27	5.1379
1128.76	1128.74	25	6	20	25	7	19	3.0759	1133.55	1133.53	26	1	25	27	2	26	5.2657
	1128.80	24	6	18	24	7	17	3.1595		1133.57	16	2	14	17	3	15	2.8738
1129.01	1128.97	21	6	16	21	7	15	3.3104	1133.84	1133.85	27	1	27	28	0	28	7.4758
	1129.02	20	6	14	20	7	13	3.3208	1134.01	1133.98	35	4	32	35	5	31	2.2929
1129.09	1129.08	19	6	14	19	7	13	3.3080	1134.32	1134.32	35	3	33	35	4	32	2.1068
	1129.10	5	5	1	6	6	0	3.7091		1134.36	14	2	12	15	3	13	2.8689
	1129.12	34	0	34	35	1	35	5.0338	1134.42	1134.47	33	4	30	33	5	29	2.6879
1129.21	1129.16	10	4	6	11	5	7	3.4337	1134.57	1134.54	7	3	5	8	4	4	3.0191
	1129.23	33	2	32	34	1	33	3.9284	1134.67	1134.66	24	1	23	25	2	24	5.4181
1129.32	1129.27	15	6	10	15	7	9	2.9860	1134.82	1134.86	31	4	28	31	5	27	3.0826
	1129.31	14	6	8	14	7	7	2.8287	1134.92	1134.95	25	2	24	26	1	25	5.3532
	1129.35	13	6	8	13	7	7	2.6368	1135.14	1135.18	25	1	25	26	0	26	8.0512
1129.40	1129.39	12	6	6	12	7	5	2.4081	1135.23	1135.20	6	3	3	7	4	4	3.0408
	1129.43	11	6	6	11	7	5	2.1399		1135.26	12	2	10	13	3	11	2.8578
1129.48	1129.46	10	6	4	10	7	3	1.8285	1135.34	1135.31	33	3	31	33	4	30	2.5510
	1129.49	9	6	4	9	7	3	1.4691		1135.38	27	4	24	27	5	23	3.8003
1129.60	1129.58	40	1	39	40	2	38	0.8816		1135.39	31	2	30	31	3	29	2.3144
1129.75	1129.77	32	1	31	33	2	32	4.1613	1135.52	1135.56	25	4	22	25	5	21	4.0872
1129.83	1129.81	33	1	33	34	0	34	5.3914	1135.65	1135.69	23	4	20	23	5	19	4.3029
	1129.83	9	4	6	10	5	5	3.4519	1135.80	1135.76	28	0	28	28	1	27	1.6375
1130.01	1130.01	14	3	11	15	4	12	3.0600		1135.80	24	0	24	25	1	25	8.2956
1130.48	1130.48	32	0	32	33	1	33	5.7515	1135.96	1135.95	20	4	16	20	5	15	4.4697
	1130.49	8	4	4	9	5	5	3.4370	1136.17	1136.16	11	4	8	11	5	7	3.3022
1130.61	1130.63	31	2	30	32	1	31	4.3889	1136.44	1136.48	23	2	22	24	1	23	5.4102
1130.69	1130.68	41	5	37	41	6	36	1.2360	1136.51	1136.51	23	1	23	24	0	24	8.5048
1131.12	1131.07	30	1	29	31	2	30	4.6025	1136.60	1136.58	29	2	28	29	3	27	2.7615
	1131.12	24	2	22	25	3	23	2.9581	1136.84	1136.87	30	4	26	30	5	25	3.5014
	1131.17	31	1	31	32	0	32	6.1118	1136.94	1136.95	29	3	27	29	4	26	3.5089
1131.25	1131.27	12	3	9	13	4	10	3.1494	1137.05	1137.04	25	3	23	26	2	24	2.7784
1131.48	1131.48	15	2	14	16	3	13	2.1278		1137.09	22	0	22	23	1	23	8.6727
1131.60	1131.55	35	5	31	36	6	30	2.1061	1137.26	1137.31	32	4	28	32	5	27	3.2221
1131.69	1131.69	22	2	20	23	3	21	2.9339	1137.41	1137.42	8	2	6	9	3	7	2.7337
1131.81	1131.83	30	0	30	31	1	31	6.4680		1137.44	30	1	29	30	2	28	2.6369
1131.90	1131.87	11	3	9	12	4	8	3.1641	1137.51	1137.53	18	1	17	19	2	18	4.9322
1132.03	1131.98	29	5	25	29	6	24	3.0515	1137.66	1137.69	27	2	26	27	3	25	3.2391
	1132.03	39	3	37	39	4	36	1.3610	1137.81	1137.83	21	1	21	22	0	22	8.7953
	1132.04	29	2	28	30	1	29	4.8037	1137.92	1137.88	7	2	6	8	3	5	2.6373
1132.24	1132.19	25	5	21	25	6	20	3.5706	1138.12	1138.10	21	2	20	22	1	21	5.2795
	1132.21	26	5	21	26	6	20	3.4612		1138.15	36	4	32	36	5	31	2.6508
	1132.27	24	5	19	24	6	18	3.6708	1138.32	1138.33	16	1	15	17	2	16	4.5275
	1132.28	23	5	19	23	6	18	3.7510		1138.35	20	0	20	21	1	21	8.8682

TABLE III (Continued)

Line Position (in cm^{-1})		Quantum Numbers							Line Position (in cm^{-1})		Quantum Numbers						
Exptl.	Theor.	J'	K'_{-1}	K'_1	J"	K''_{-1}	K''_1	$\frac{I^\circ_{n''n'}}{C'}$	Exptl.	Theor.	J'	K'_{-1}	K'_1	J"	K''_{-1}	K''_1	$\frac{I^\circ_{n''n'}}{C'}$
1138.41	1138.42	34	2	32	34	3	31	2.6986	1145.76	1145.72	7	1	7	7	2	6	2.9065
1138.67	1138.64	6	2	4	7	3	5	2.5886		1145.78	18	1	17	18	2	16	7.6320
	1138.71	25	2	24	25	3	23	3.7254	1146.07	1146.08	6	0	6	7	1	7	4.0047
1138.84	1138.85	21	3	19	21	4	18	4.9279		1146.10	5	1	5	5	2	4	2.2487
1139.14	1139.09	19	3	17	19	4	16	5.0126	1146.29	1146.25	16	4	12	15	5	11	1.1381
	1139.11	14	1	13	15	2	14	4.0803		1146.29	27	5	23	28	4	24	1.1181
	1139.15	19	1	19	20	0	20	8.8828	1146.39	1146.36	3	1	3	3	2	2	1.3572
1139.52	1139.48	13	3	11	13	4	10	4.3838		1146.43	22	5	17	21	6	16	1.0973
	1139.55	11	3	9	11	4	8	3.8750	1146.62	1146.59	2	1	1	2	2	0	0.8270
1139.61	1139.59	18	0	18	19	1	19	8.8436	1146.81	1146.84	17	4	14	16	5	11	1.1990
	1139.65	7	3	5	7	4	4	2.4019	1146.99	1147.02	21	4	18	22	3	19	1.5497
1139.85	1139.85	18	3	15	18	4	14	5.1505	1147.09	1147.05	12	0	12	12	1	11	5.1220
1140.03	1140.03	32	2	30	32	3	29	3.4571		1147.12	12	1	11	12	2	10	7.4668
	1140.07	27	4	24	28	3	25	1.4616	1147.16	1147.16	10	1	9	10	2	8	6.3111
1140.42	1140.42	21	2	20	21	3	19	4.5928	1147.46	1147.47	7	2	6	6	3	3	0.6133
	1140.44	22	3	19	22	4	18	5.3365		1147.50	18	4	14	17	5	13	1.2488
1140.55	1140.55	3	2	2	4	3	1	2.3031	1147.68	1147.67	7	7	1	8	0	8	4.0908
1140.70	1140.73	26	1	25	26	2	24	3.9157	1147.81	1147.83	15	3	13	16	2	14	1.8796
1141.01	1141.03	19	1	19	19	2	18	3.0150	1148.03	1148.01	10	0	10	10	1	9	5.5528
1141.11	1141.10	19	2	18	19	3	17	4.8900		1148.05	19	4	16	18	5	13	1.2823
1141.20	1141.18	26	3	23	26	4	22	5.2910	1148.18	1148.17	2	0	2	3	1	3	1.9475
	1141.20	2	2	0	3	3	1	2.2393		1148.21	25	5	21	24	6	18	1.0752
1141.38	1141.37	32	3	29	32	4	28	4.3161	1148.28	1148.28	25	5	21	26	4	22	1.2159
1141.48	1141.44	30	2	28	30	3	27	4.3615	1148.49	1148.48	26	5	21	27	4	24	1.1349
	1141.44	28	3	25	28	4	24	5.1249	1148.61	1148.58	14	3	11	13	4	10	1.2668
	1141.53	30	3	27	30	4	26	4.8040	1148.75	1148.75	8	0	8	8	1	7	5.6104
1141.84	1141.85	15	1	15	16	0	16	8.3027		1148.77	20	4	16	19	5	15	1.3084
1141.93	1141.94	14	0	14	15	1	15	8.0252	1148.87	1148.88	26	5	21	25	6	20	1.0533
1142.10	1142.08	17	1	17	17	2	16	3.2916	1148.98	1148.97	9	2	8	10	1	9	1.9883
	1142.11	15	2	14	15	3	13	5.0050	1149.18	1149.18	5	1	5	6	0	6	2.8037
1142.33	1142.37	24	1	23	24	2	22	4.7593	1149.27	1149.29	6	0	6	6	1	5	5.1109
1142.43	1142.46	13	2	12	13	3	11	4.7709	1149.41	1149.40	27	5	23	26	6	20	1.0221
1142.52	1142.53	6	1	5	7	2	6	2.3426	1149.72	1149.72	11	2	10	10	3	7	1.1804
1142.72	1142.71	11	2	10	11	3	9	4.3361	1149.83	1149.86	2	0	2	2	1	1	2.4036
1143.00	1143.00	7	2	6	7	3	5	2.9282	1150.16	1150.14	17	3	15	16	4	12	1.4377
	1143.03	15	1	15	15	2	14	3.5021	1150.26	1150.28	16	3	13	17	2	16	1.2610
	1143.04	12	0	12	13	1	13	7.2264	1150.72	1150.73	7	2	6	8	1	7	1.4153
1143.12	1143.12	18	0	18	18	1	17	3.4440	1150.88	1150.90	17	4	14	18	3	15	1.5217
	1143.17	8	2	6	8	3	5	3.4007	1151.09	1151.11	14	3	11	15	2	14	1.3597
1143.22	1143.24	13	1	13	14	0	14	7.5874	1151.24	1151.22	19	3	17	18	4	14	1.4650
1143.34	1143.30	10	2	8	10	3	7	4.2219		1151.26	12	2	10	11	3	9	1.4125
1143.54	1143.50	12	2	10	12	3	9	4.9900	1151.45	1151.45	18	3	15	17	4	14	1.5178
	1143.56	4	1	3	5	2	4	1.9394	1151.55	1151.54	15	2	14	14	3	11	1.3504
1143.76	1143.78	14	2	12	14	3	11	5.7326		1151.57	25	4	22	24	5	19	1.2357
	1143.79	3	1	3	4	2	2	1.5901	1152.02	1152.06	1	1	1	2	0	2	0.5152
1143.88	1143.88	13	1	13	13	2	12	3.6079	1152.20	1152.16	17	2	16	16	3	13	1.2543
1144.08	1144.03	24	2	22	24	3	21	7.0346		1152.21	21	3	19	20	4	16	1.4165
	1144.06	16	2	14	16	3	13	6.4419	1152.40	1152.39	8	1	7	7	2	6	1.4213
1144.27	1144.30	18	2	16	18	3	15	7.0459		1152.40	5	2	4	6	1	5	0.8794
1144.37	1144.34	22	2	20	22	3	19	7.4290	1152.53	1152.52	19	2	18	18	3	15	1.0645
	1144.41	20	2	18	20	3	17	7.4164	1152.62	1152.60	4	0	4	3	1	3	1.6167
1144.64	1144.61	11	1	11	11	2	10	3.5673		1152.66	27	4	24	26	5	21	1.1383
	1144.68	11	1	11	12	0	12	6.5969	1152.75	1152.79	20	5	15	21	4	18	1.3376
1144.82	1144.84	20	1	19	20	2	18	6.7459	1153.05	1153.01	26	4	22	25	5	21	1.2263
1145.08	1145.08	8	0	8	9	1	9	5.1188		1153.06	20	3	17	19	4	16	1.5669
1145.28	1145.27	9	1	9	9	2	8	3.3423	1153.21	1153.24	10	3	7	11	2	10	1.1990
	1145.29	13	2	12	14	1	13	3.2313	1153.32	1153.30	9	3	7	10	2	8	1.1368
1145.63	1145.62	15	4	12	14	5	9	1.0631	1153.46	1153.43	2	1	1	2	0	2	2.4317

TABLE III (Continued)

Line Position (in cm^{-1})		Quantum Numbers							Line Position (in cm^{-1})		Quantum Numbers						
Exptl.	Theor.	J'	K'_{-1}	K'_1	J"	K''_{-1}	K''_1	$\frac{I^{\circ}_{n''n'}}{C'}$	Exptl.	Theor.	J'	K'_{-1}	K'_1	J"	K''_{-1}	K''_1	$\frac{I^{\circ}_{n''n'}}{C'}$
1153.57	1153.60	4	1	3	4	0	4	4.0585	1161.46	1161.48	9	2	8	8	1	7	2.9454
1153.68	1153.68	14	4	10	15	3	13	1.3623	1161.65	1161.67	17	1	17	16	0	16	9.1805
1153.87	1153.89	6	1	5	6	0	6	5.1828	1161.79	1161.75	28	2	26	28	1	27	3.4262
1153.99	1154.01	6	0	6	5	1	5	2.8458	1161.96	1161.94	20	4	16	20	3	17	5.6210
	1154.03	10	1	9	9	2	8	2.0182	1162.24	1162.23	11	2	10	10	1	9	3.4213
1154.22	1154.18	13	4	10	14	3	11	1.2948	1162.58	1162.55	36	3	33	36	2	34	2.2427
	1154.24	18	5	13	19	4	16	1.3158	1162.71	1162.67	19	1	19	18	0	18	9.5430
1154.32	1154.33	8	1	7	8	0	8	5.7021		1162.73	4	3	1	3	2	2	2.4772
1154.48	1154.45	8	3	5	9	2	8	0.9528		1162.75	32	5	27	32	4	28	3.4451
1154.81	1154.82	22	3	19	21	4	18	1.5819	1162.97	1162.97	23	2	22	23	1	23	2.5725
1154.92	1154.90	17	5	13	18	4	14	1.2858		1162.99	20	0	20	19	1	19	9.6043
	1154.96	10	1	9	10	0	10	5.6626	1163.08	1163.07	30	2	28	30	1	29	2.8387
1155.10	1155.10	3	1	3	2	0	2	1.9924		1163.10	19	4	16	19	3	17	5.3980
1155.47	1155.44	8	0	8	7	1	7	4.1914	1163.36	1163.32	13	4	10	13	3	11	4.7295
1155.77	1155.75	14	2	12	14	1	13	8.3110		1163.34	5	3	3	4	2	2	2.5867
	1155.81	10	2	8	10	1	9	6.4671		1163.36	27	3	25	27	2	26	3.5012
1155.96	1156.00	16	2	14	16	1	15	8.3573	1163.48	1163.45	27	4	24	27	3	25	4.2901
1156.25	1156.28	6	2	4	6	1	5	3.5471		1163.51	15	2	14	14	1	13	4.4284
1156.52	1156.52	4	2	2	4	1	3	2.1798	1163.67	1163.68	21	1	21	20	0	20	9.6395
	1156.55	18	2	16	17	3	15	2.1532	1164.12	1164.08	22	0	22	21	1	21	9.5864
1156.78	1156.78	14	1	13	14	0	14	4.6794		1164.09	17	2	16	16	1	15	4.9375
1156.88	1156.85	10	0	10	9	1	9	5.5801	1164.36	1164.35	28	5	23	28	4	24	4.0897
	1156.92	3	2	2	3	1	3	1.4049	1164.52	1164.54	7	3	5	6	2	4	2.8192
1157.09	1157.08	7	1	7	6	0	6	4.1544	1164.71	1164.68	19	2	18	18	1	17	5.4038
	1157.12	5	2	4	5	1	5	2.3308		1164.69	23	1	23	22	0	22	9.4980
1157.38	1157.38	22	3	19	22	2	20	7.6736	1164.98	1164.98	26	5	21	26	4	22	4.3905
	1157.39	24	3	21	24	2	22	7.2681	1165.08	1165.10	24	1	23	23	2	22	5.9336
	1157.42	14	1	13	13	2	12	3.3537	1165.18	1165.14	24	0	24	23	1	23	9.3436
1157.56	1157.58	20	3	17	20	2	18	7.6701		1165.20	35	4	32	35	3	33	2.3080
1157.69	1157.66	26	3	23	26	2	24	6.5140	1165.34	1165.32	21	2	20	20	1	19	5.7718
1157.89	1157.93	16	1	15	16	0	16	4.1120		1165.37	24	5	19	24	4	20	4.6456
1158.05	1158.08	22	2	20	22	1	21	5.9510	1165.50	1165.52	35	5	31	35	4	32	2.5137
1158.20	1158.18	28	3	25	28	2	26	5.5542	1165.73	1165.71	25	1	25	24	0	24	9.1533
	1158.20	12	0	12	11	1	11	6.8886	1165.82	1165.83	25	5	21	25	4	22	4.4831
1158.41	1158.41	16	3	13	16	2	14	6.7027		1165.86	22	5	17	22	4	18	4.8266
1158.63	1158.62	32	4	28	32	3	29	4.4930	1165.93	1165.97	28	2	26	27	3	25	3.1423
1158.89	1158.86	11	1	11	10	0	10	6.5417	1166.20	1166.18	26	0	26	25	1	25	8.9146
	1158.89	14	3	11	14	2	12	5.9887	1166.31	1166.35	26	1	25	25	2	24	5.9280
1159.16	1159.16	18	1	17	18	0	18	3.6090	1166.67	1166.64	15	5	11	15	4	12	4.5809
1159.32	1159.33	28	4	24	28	3	25	5.3551		1166.69	14	5	9	14	4	10	4.4081
	1159.34	12	3	9	12	2	10	5.2332		1166.72	27	1	27	26	0	26	8.6456
1159.48	1159.48	42	5	37	42	4	38	1.7129	1167.00	1166.99	6	5	1	6	4	2	1.4387
	1159.49	14	0	14	13	1	13	7.9961	1167.20	1167.18	34	3	31	33	4	30	1.5014
1159.57	1159.57	15	2	14	15	1	15	3.6894		1167.20	28	0	28	27	1	27	8.3422
1159.68	1159.67	5	2	4	4	1	3	2.0449	1167.33	1167.31	34	6	28	34	5	29	2.5443
	1159.69	10	3	7	10	2	8	4.4423	1167.43	1167.40	6	4	2	5	3	3	3.3127
1159.78	1159.77	13	1	13	12	0	12	7.6408	1167.52	1167.51	28	1	27	27	2	26	5.7414
1160.04	1160.01	32	3	29	32	2	30	3.6337		1167.55	13	3	11	12	2	10	3.1802
1160.30	1160.27	38	5	33	38	4	34	2.4571	1167.72	1167.72	29	1	29	28	0	28	8.0155
	1160.32	13	3	11	13	2	12	5.0457		1167.75	37	6	32	37	5	33	1.9992
1160.46	1160.43	20	1	19	20	0	20	3.1720	1167.95	1167.94	12	3	9	11	2	10	2.9401
	1160.48	15	3	13	15	2	14	5.2988		1167.98	35	6	30	35	5	31	2.3469
1160.71	1160.71	16	0	16	15	1	15	8.8276	1168.20	1168.21	30	0	30	29	1	29	7.6665
	1160.75	18	1	17	17	2	16	4.7414	1168.29	1168.27	15	3	13	14	2	12	3.2105
1161.03	1161.00	36	5	31	36	4	32	2.8004	1168.38	1168.37	30	6	24	30	5	25	3.2499
	1161.07	19	3	17	19	2	18	5.1981	1168.52	1168.50	29	2	28	28	1	27	5.6145
1161.18	1161.16	19	2	18	19	1	19	3.2117	1168.61	1168.61	30	1	29	29	2	28	5.4144
	1161.22	34	3	31	34	2	32	2.8615	1168.75	1168.72	31	1	31	30	0	30	7.3027

TABLE III (Continued)

Line Position (in cm^{-1})		Quantum Numbers							Line Position (in cm^{-1})		Quantum Numbers						
Exptl.	Theor.	J'	K'_{-1}	K'_1	J"	K''_{-1}	K''_1	$\frac{I^{\circ}_{n''n'}}{C'}$	Exptl.	Theor.	J'	K'_{-1}	K'_1	J"	K''_{-1}	K''_1	$\frac{I^{\circ}_{n''n'}}{C'}$
	1168.76	28	6	22	28	5	23	3.5837	1176.76	1176.76	18	8	10	18	7	11	3.2214
	1168.77	29	6	24	29	5	25	3.4167	1177.07	1177.06	12	8	4	12	7	5	2.1942
1168.98	1169.02	27	6	22	27	5	23	3.7363		1177.10	11	8	4	11	7	5	1.8783
1169.22	1169.21	32	0	32	31	1	31	6.9266	1177.20	1177.17	49	1	49	48	0	48	1.5961
	1169.26	25	6	20	25	5	21	4.0100	1177.32	1177.30	11	6	6	10	5	5	4.2495
1169.32	1169.33	24	6	18	24	5	19	4.1240	1177.41	1177.38	17	5	13	16	4	12	3.7067
1169.54	1169.55	22	6	16	22	5	17	4.2921		1177.40	22	4	18	21	3	19	2.5615
1169.63	1169.66	21	6	16	21	5	17	4.3254	1177.90	1177.90	12	6	6	11	5	7	4.2210
	1169.67	32	1	31	31	2	30	4.9883	1178.25	1178.28	7	7	1	6	6	0	4.6161
1169.80	1169.82	19	6	14	19	5	15	4.3617	1178.43	1178.44	36	9	27	36	8	28	1.4496
1169.94	1169.96	17	6	12	17	5	13	4.2603	1178.60	1178.58	35	9	27	35	8	28	1.5651
1170.10	1170.08	15	6	10	15	5	11	4.0216	1178.90	1178.89	8	7	1	7	6	2	4.5529
1170.20	1170.19	13	6	8	13	5	9	3.6306		1178.94	24	4	20	23	3	21	2.1524
	1170.19	34	0	34	33	1	33	6.1576	1178.99	1178.96	32	9	23	32	8	24	1.9216
	1170.23	12	6	6	12	5	7	3.3512	1179.46	1179.49	27	9	19	27	8	20	2.4697
1170.31	1170.27	25	3	23	24	2	22	3.3749		1179.50	9	7	3	8	6	2	4.5036
	1170.27	11	6	6	11	5	7	3.0034	1179.55	1179.54	21	5	17	20	4	16	3.2311
	1170.31	10	6	4	10	5	5	2.7237		1179.58	26	9	17	26	8	18	2.5204
	1170.34	33	2	32	32	1	31	4.7563	1179.68	1179.67	25	9	17	25	8	18	2.6054
1170.65	1170.68	35	1	35	34	0	34	5.7715		1179.68	15	6	10	14	5	9	4.0589
1171.03	1171.05	12	4	8	11	3	9	3.6027	1179.81	1179.83	23	9	15	23	8	16	2.7489
1171.19	1171.16	36	0	36	35	1	35	5.3892	1180.05	1180.04	20	9	11	20	8	12	2.7809
1171.29	1171.28	35	2	34	34	1	33	4.2481	1180.29	1180.26	16	6	10	15	5	11	3.9776
1171.40	1171.44	7	5	3	6	4	2	3.8878		1180.28	16	9	7	16	8	8	2.4752
1171.50	1171.53	34	7	27	34	6	28	2.2343		1180.33	15	9	7	15	8	8	2.3212
1171.60	1171.64	37	1	37	36	0	36	5.0134	1180.69	1180.71	11	7	5	10	6	4	4.4112
1171.76	1171.77	33	7	27	33	6	28	2.3927	1181.34	1181.32	12	7	5	11	6	6	4.3578
1171.86	1171.88	33	3	31	32	2	30	3.0935		1181.37	24	5	19	23	4	20	2.7568
1172.09	1172.05	8	5	3	7	4	4	3.9194	1181.89	1181.91	13	7	7	12	6	6	4.2958
	1172.12	38	0	38	37	1	37	4.6462	1181.99	1181.99	19	6	14	18	5	13	3.6572
1172.22	1172.17	30	7	23	30	6	24	2.8660	1182.26	1182.29	33	10	24	33	9	25	1.5309
	1172.22	37	2	36	36	1	35	3.7267		1182.30	8	8	0	7	7	1	4.7038
	1172.25	14	4	10	13	3	11	3.5585	1182.40	1182.40	32	10	22	32	9	23	1.6311
1172.55	1172.51	35	3	33	34	2	32	2.8587	1182.53	1182.51	14	7	7	13	6	8	4.2237
	1172.55	27	7	21	27	6	22	3.2991		1182.51	31	10	22	31	9	23	1.7294
	1172.59	39	1	39	38	0	38	4.2906		1182.56	20	6	14	19	5	15	3.5277
1173.04	1173.04	22	7	15	22	6	16	3.7692	1182.63	1182.61	30	10	20	30	9	21	1.8259
	1173.06	40	0	40	39	1	39	3.9477	1182.77	1182.77	29	5	25	28	4	24	1.9713
1173.15	1173.12	21	7	15	21	6	16	3.8155		1182.81	28	10	18	28	9	19	2.0047
	1173.16	39	2	38	38	1	37	3.2142	1182.93	1182.90	27	10	18	27	9	19	2.0873
1173.33	1173.34	18	7	11	18	6	12	3.7734		1182.91	9	8	2	8	7	1	4.6166
1173.53	1173.51	15	7	9	15	6	10	3.4216	1183.05	1183.07	25	10	16	25	9	17	2.2155
	1173.53	41	1	41	40	0	40	3.6193	1183.18	1183.15	24	10	14	24	9	15	2.2634
	1173.56	14	7	7	14	6	8	3.2679	1183.50	1183.50	19	10	10	19	9	11	2.2419
1173.99	1174.00	42	0	42	41	1	41	3.3067		1183.52	10	8	2	9	7	3	4.5394
1174.18	1174.19	34	8	26	34	7	27	1.9510	1183.70	1183.68	22	6	16	21	5	17	3.2426
1174.49	1174.47	12	5	7	11	4	8	3.9738		1183.69	16	7	9	15	6	10	4.0463
	1174.52	19	4	16	18	3	15	3.1785	1184.23	1184.21	23	6	18	22	5	17	3.0900
1174.73	1174.70	18	4	14	17	3	15	3.2146		1184.27	17	7	11	16	6	10	3.9408
1175.01	1175.01	43	2	42	42	1	41	2.7294	1184.69	1184.72	12	8	4	11	7	5	4.3880
1175.18	1175.19	34	8	26	34	7	27	1.9510	1184.78	1184.77	24	6	18	23	5	19	2.9318
1175.36	1175.33	33	8	26	33	7	27	2.0896	1184.89	1184.85	18	7	11	17	6	12	3.8250
	1175.38	45	1	45	44	0	44	2.4696	1185.30	1185.32	13	8	6	12	7	5	4.3060
1175.72	1175.71	30	8	22	30	7	23	2.5023	1185.40	1185.43	19	7	13	18	6	12	3.6993
1175.90	1175.94	28	8	20	28	7	21	2.7590	1185.87	1185.85	26	6	20	25	5	21	2.6066
1175.99	1176.00	20	4	16	19	3	17	2.9217	1186.01	1186.00	20	7	13	19	6	14	3.5649
1176.40	1176.38	27	4	24	26	3	23	2.2570		1186.01	30	11	19	30	10	20	1.5172
	1176.41	23	8	16	23	7	17	3.2253	1186.14	1186.11	29	11	19	29	10	20	1.5953
1176.62	1176.63	20	8	12	20	7	13	3.2975	1186.23	1186.20	28	11	17	28	10	18	1.6644

TABLE III (Continued)

Line Position (in cm^{-1})		Quantum Numbers							Line Position (in cm^{-1})		Quantum Numbers						
Exptl.	Theor.	J'	K'_{-1}	K'_{1}	J"	K''_{-1}	K''_{1}	$\frac{I^{\circ}_{n''n'}}{C'}$	Exptl.	Theor.	J'	K'_{-1}	K'_{1}	J"	K''_{-1}	K''_{1}	$\frac{I^{\circ}_{n''n'}}{C'}$
1186.53	1186.51	15	8	8	14	7	7	4.1196	1193.35	1193.32	15	10	6	14	9	5	3.8143
	1186.54	24	11	13	24	10	14	1.8513		1193.33	27	8	20	26	7	19	2.4321
	1186.57	21	7	15	20	6	14	3.4270		1193.38	22	13	9	22	12	10	1.1629
1187.23	1187.27	29	6	24	28	5	23	2.1184	1193.61	1193.63	18	13	5	18	12	6	0.9632
1187.47	1187.52	11	9	3	10	8	2	4.4136	1193.71	1193.73	16	13	3	16	12	4	0.7488
1187.68	1187.69	17	8	10	16	7	9	3.8988	1193.87	1193.88	28	8	20	27	7	21	2.2700
1187.97	1187.96	30	6	24	29	5	25	1.9559		1193.89	16	10	6	15	9	7	3.6923
1188.12	1188.12	12	9	3	11	8	4	4.3169	1194.25	1194.27	11	11	1	10	10	0	4.0346
1188.24	1188.24	24	7	17	23	6	18	2.9621	1194.46	1194.41	29	8	22	28	7	21	2.1156
	1188.27	18	8	10	17	7	11	3.7756		1194.48	17	10	8	16	9	7	3.5695
1188.70	1188.72	13	9	5	12	8	4	4.2182	1194.88	1194.88	12	11	1	11	10	2	3.9127
1188.95	1188.98	33	6	28	32	5	27	1.5117	1195.06	1195.06	18	10	8	17	9	9	3.4404
1189.26	1189.29	31	12	20	31	11	21	1.1782		1195.10	24	9	15	23	8	16	2.7745
1189.36	1189.32	14	9	5	13	8	6	4.1153	1195.43	1195.47	31	8	24	30	7	23	1.8284
	1189.39	30	12	18	30	11	19	1.2443		1195.48	13	11	3	12	10	2	3.7940
1189.52	1189.48	29	12	18	29	11	19	1.3025	1195.64	1195.64	19	10	10	18	9	9	3.3070
	1189.57	28	12	16	28	11	17	1.3560		1195.66	25	9	17	24	8	16	2.6211
1189.73	1189.74	26	12	14	26	11	15	1.4432	1195.99	1195.99	32	8	24	31	7	25	1.6755
1189.83	1189.82	25	12	14	25	11	15	1.4742	1196.22	1196.21	26	9	17	25	8	18	2.4751
	1189.87	27	7	21	26	6	20	2.4777		1196.22	20	10	10	19	9	11	3.1695
1189.93	1189.90	24	12	12	24	11	13	1.4923	1196.47	1196.50	33	8	26	32	7	25	1.5390
	1189.91	15	9	7	14	8	6	4.0068	1196.64	1196.67	15	11	5	14	10	4	3.5567
1190.02	1189.99	21	8	14	20	7	13	3.3620	1196.98	1197.01	34	8	26	33	7	27	1.4083
	1190.04	22	12	10	22	11	11	1.4991	1197.24	1197.26	16	11	5	15	10	6	3.4352
1190.17	1190.17	20	12	8	20	11	9	1.4424	1197.34	1197.31	28	9	19	27	8	20	2.1679
1190.44	1190.41	28	7	21	27	6	22	2.3167		1197.37	22	10	12	21	9	13	2.8856
1190.58	1190.56	22	8	14	21	7	15	3.2155	1197.81	1197.85	17	11	7	16	10	6	3.3110
1191.05	1191.09	17	9	9	16	8	8	3.7706		1197.85	29	9	21	28	8	20	2.0291
1192.07	1192.11	13	10	4	12	9	3	4.0434	1197.93	1197.93	23	10	14	22	9	13	2.7406
1192.26	1192.24	25	8	18	24	7	17	2.7441	1198.06	1198.02	36	8	28	35	7	29	1.1663
	1192.25	19	9	11	18	8	10	3.5088	1198.26	1198.23	12	12	0	11	11	1	3.6096
1192.73	1192.70	14	10	4	13	9	5	3.9303	1198.42	1198.39	30	9	21	29	8	22	1.8731
1192.83	1192.79	26	8	18	25	7	19	2.5853		1198.44	18	11	7	17	10	8	3.1838
	1192.83	20	9	11	19	8	12	3.3694	1198.90	1198.92	31	9	23	30	8	22	1.7333
1192.99	1193.01	27	13	15	27	12	16	1.1176	1199.45	1199.43	14	12	2	13	11	3	3.3690
1193.09	1193.09	26	13	13	26	12	14	1.1452		1199.45	32	9	23	31	8	24	1.5983
1193.20	1193.17	25	13	13	25	12	14	1.1649	1199.58	1199.60	20	11	9	19	10	10	2.9216
	1193.24	24	13	11	24	12	12	1.1753		1199.63	26	10	16	25	9	17	2.2873

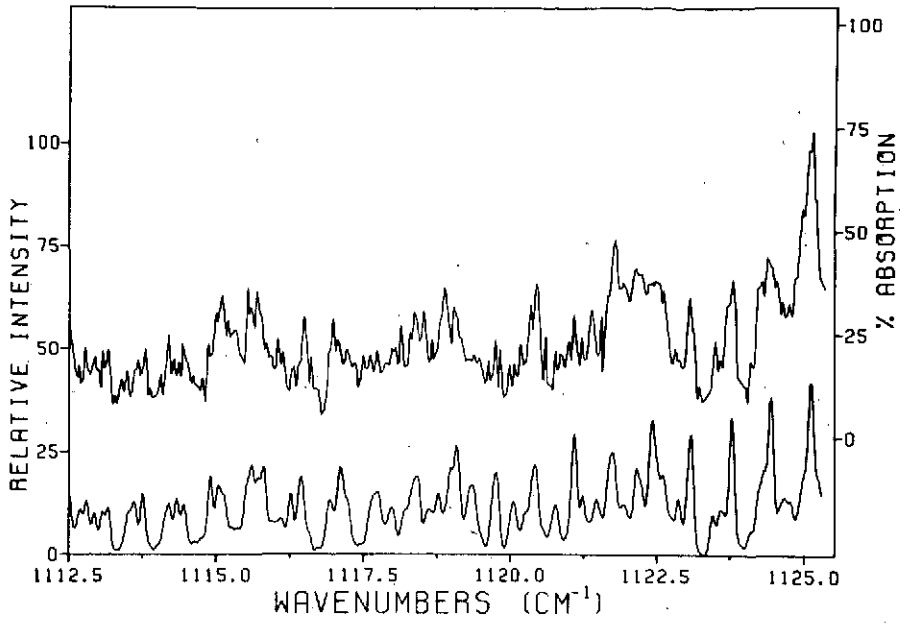

Fig. 1(a). Experimental and theoretical spectra of ν_1 band of $^{32}S^{16}O_2$ in range 1112.5 to 1125.0 cm^{-1}.

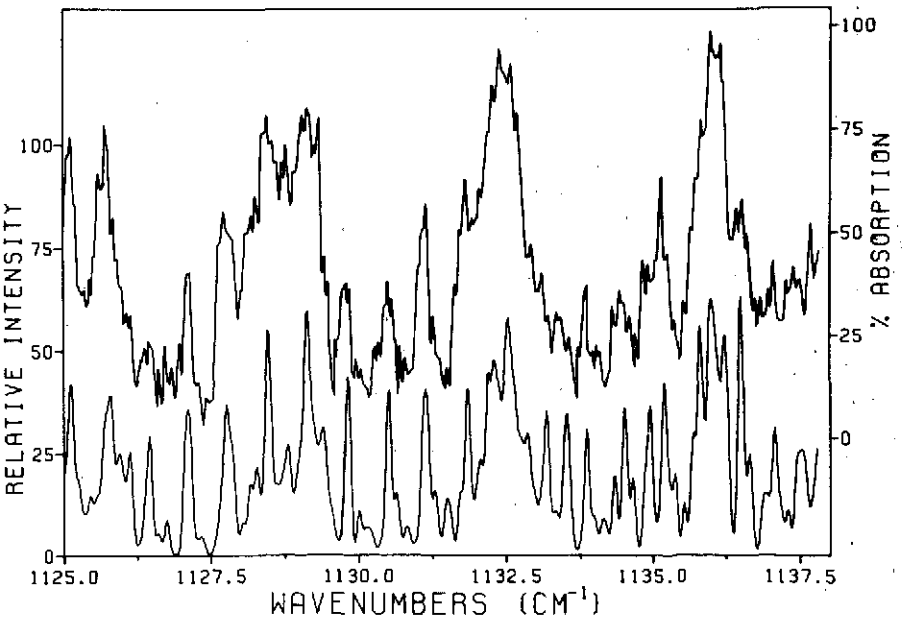

Fig. 1(b). Experimental and theoretical spectra of ν_1 band of $^{32}S^{16}O_2$ in range 1125.0 to 1137.5 cm^{-1}.

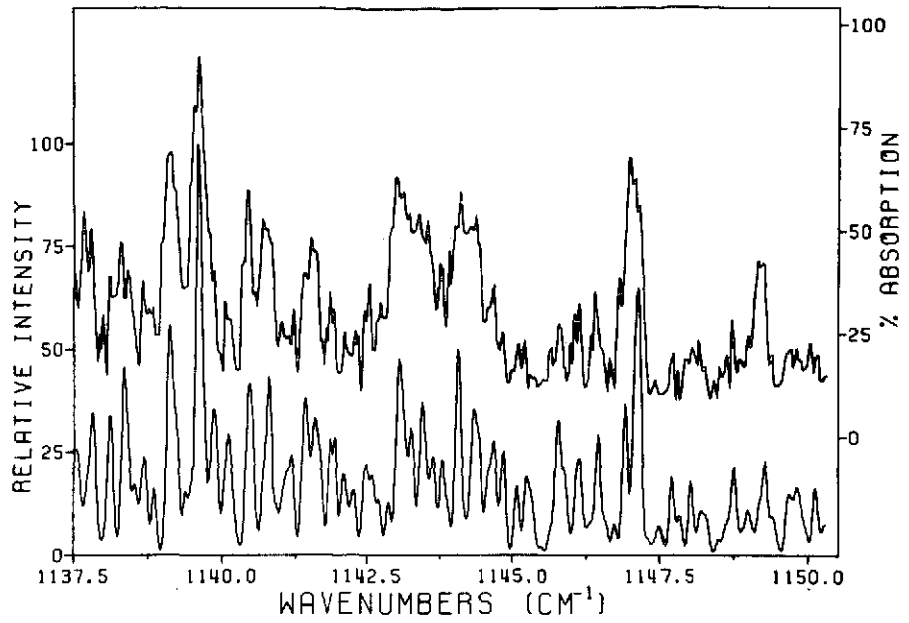

Fig. 1(c). Experimental and theoretical spectra of ν_1 band of $^{32}S^{16}O_2$ in range 1137.5 to 1150.0 cm^{-1}.

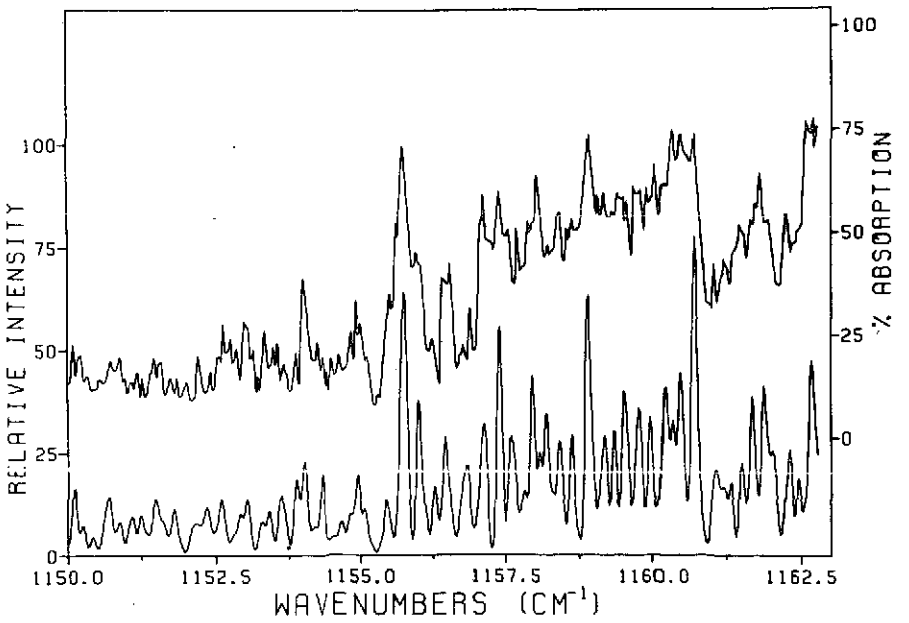

Fig. 1(d). Experimental and theoretical spectra of ν_1 band of $^{32}S^{16}O_2$ in range 1150.0 to 1162.5 cm^{-1}.

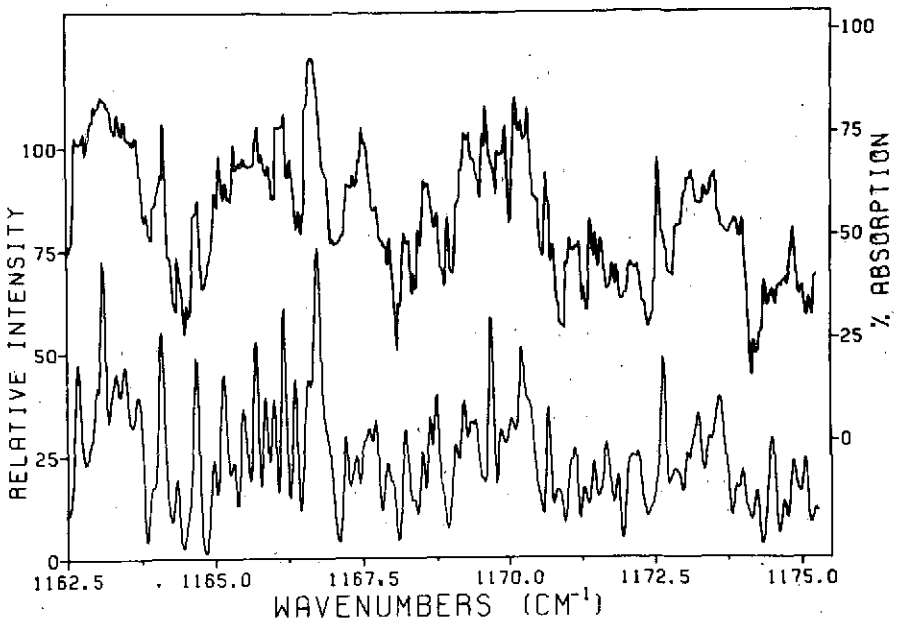

Fig. 1(e). Experimental and theoretical spectra of ν_1 band of $^{32}S^{16}O_2$ in range 1162.5 to 1175.0 cm^{-1}.

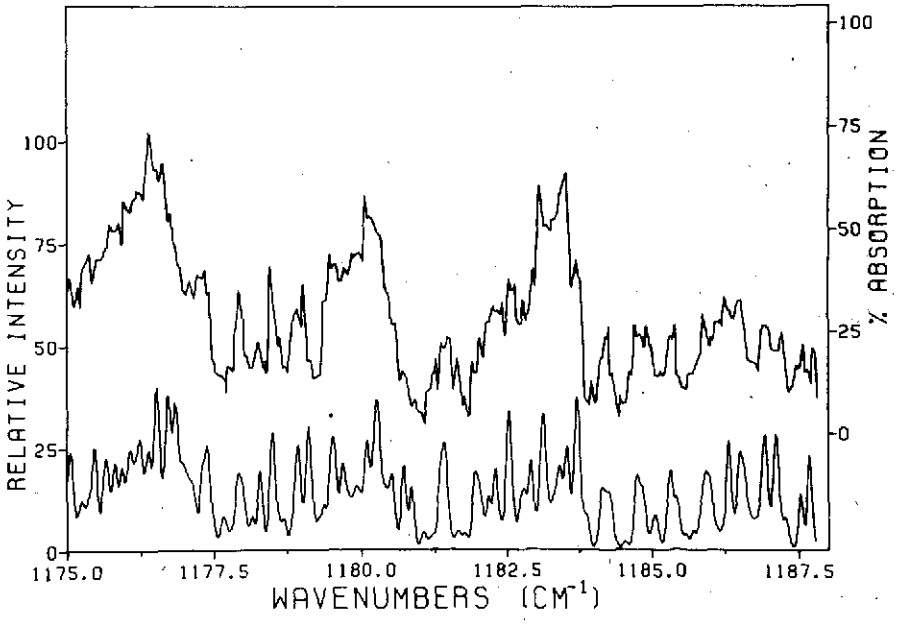

Fig. 1(f). Experimental and theoretical spectra of ν_1 band of $^{32}S^{16}O_2$ in range 1175.0 to 1187.5 cm^{-1}.

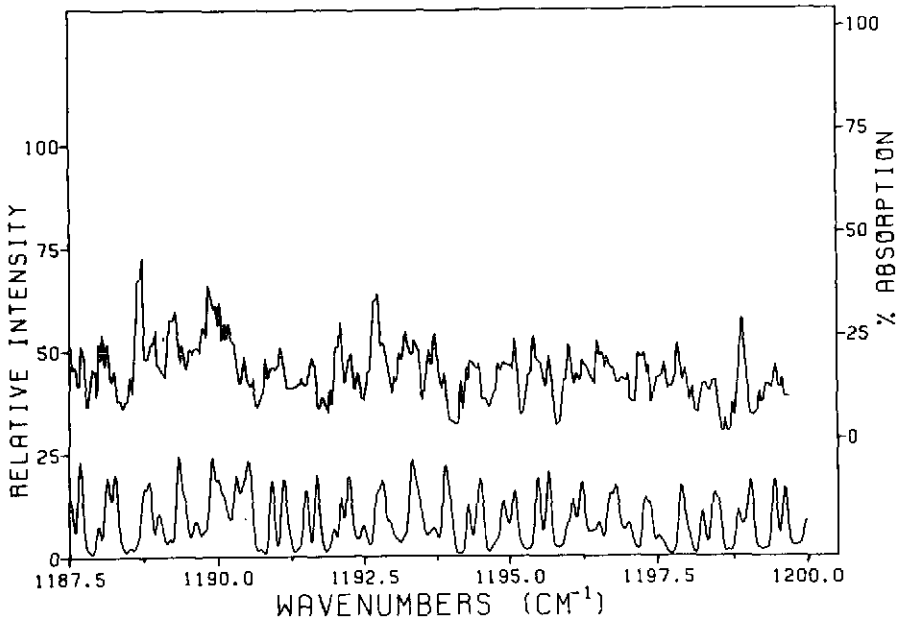

Fig. 1(g). Experimental and theoretical spectra of ν_1 band of $^{32}S^{16}O_2$ in range 1187.5 to 1200.0 cm^{-1}.

lines in Table I of Ref. 8, and have determined that the two sets of values agree to 0.01 cm^{-1} except for a single line with J = 30 for which the apparent discrepancy is only 0.02 cm^{-1}. Subsequently, from a more extensive tabulation provided by Hinkley [Appendix B of Ref. 30] we found that for all lines with $J \leq 46$, of which there are 78, the maximum difference in the calculated line positions was 0.02 cm^{-1}. These differences may be attributed to the small disparities in assumed excited-state centrifugal distortion constants.

In Fig. 2 and Table IV, we have compared our experimental and theoretical results for ν_2 in the spectral range from 470 to 590 cm^{-1}. The selection rules for this band[25] are the same as those for ν_1, described above. Because of the lower resolution available in the ν_2 region, we have been able to assign only approximately 180 observed lines. Strong well-defined peaks in Fig. 2 correspond to Q sub-branches. A sub-branch, in the case of a nearly prolate symmetric top, is characterized by a constant value of K_{-1} and the parity of the initial state. Individual lines in these sub-branches are in most cases unresolved. In Table IV, the subscripts to Q denote the changes in K_{-1} and K_1. The initial state of the transitions is given in parentheses. For low values of K_{-1}, the even- and odd-parity

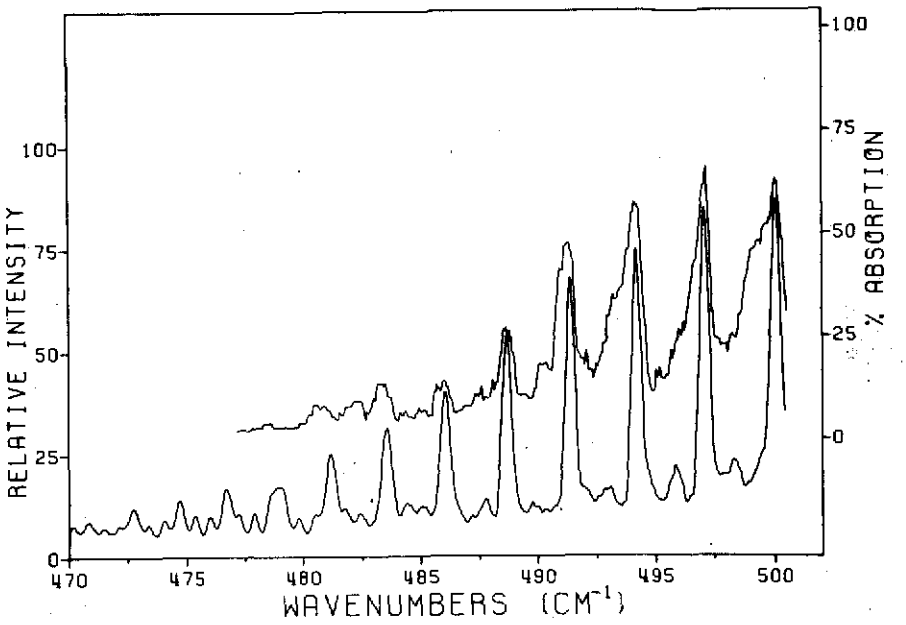

Fig. 2(a). Experimental and theoretical spectra of ν_2 band of $^{32}S^{16}O_2$ in range 470 to 500 cm^{-1}.

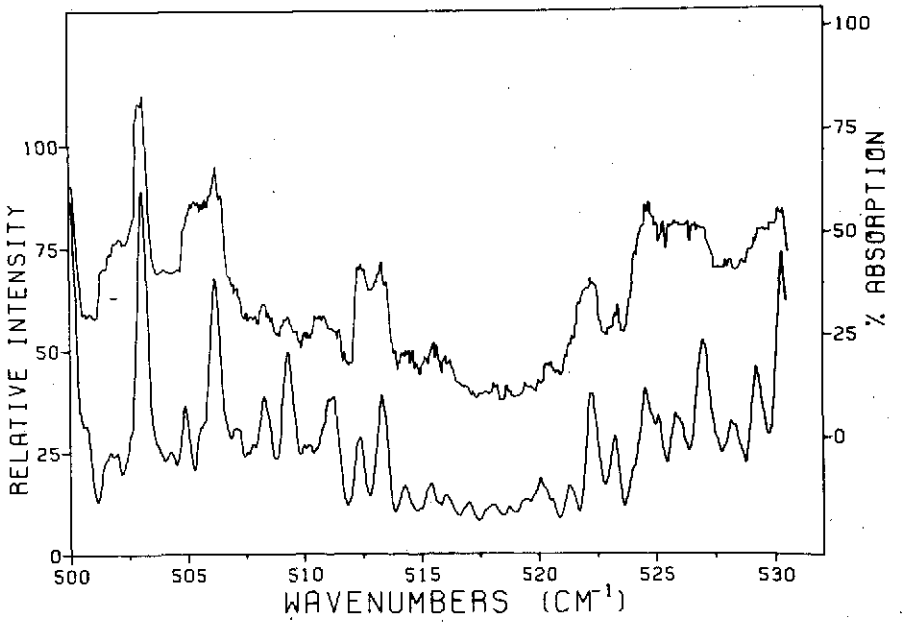

Fig. 2(b). Experimental and theoretical spectra of ν_2 band of $^{32}S^{16}O_2$ in range 500 to 530 cm^{-1}.

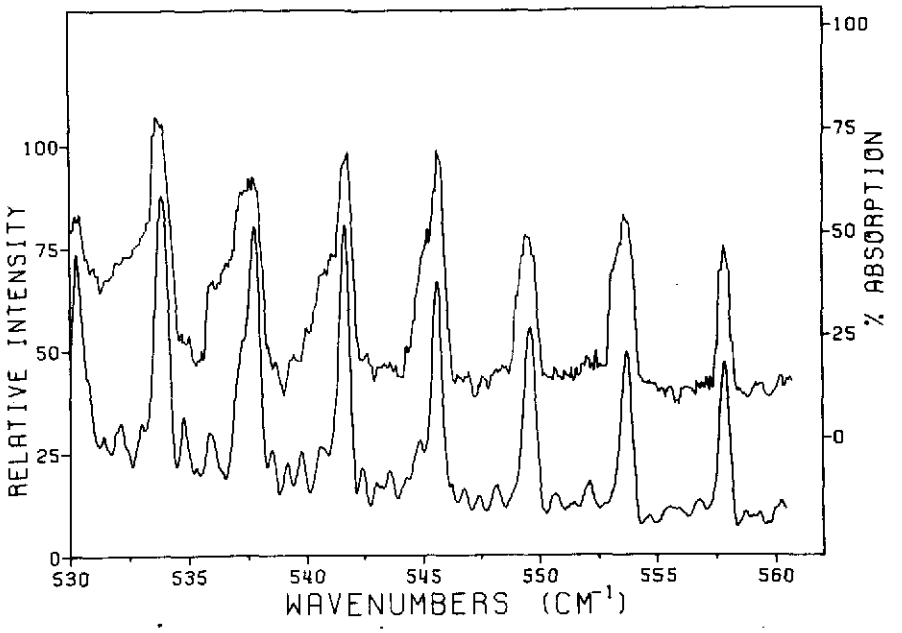

Fig. 2(c). Experimental and theoretical spectra of ν_2 band of $^{32}S^{16}O_2$ in range 530 to 560 cm^{-1}.

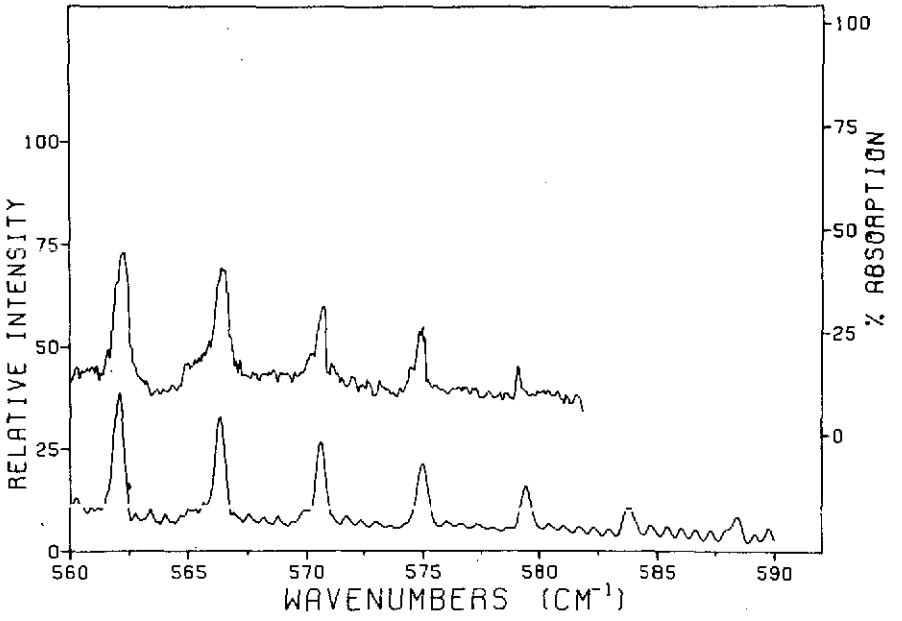

Fig. 2(d). Experimental and theoretical spectra of ν_2 band of $^{32}S^{16}O_2$ in range 560 to 590 cm^{-1}.

TABLE IV

COMPARISON OF EXPERIMENTAL AND THEORETICAL SPECTRAL LINE POSITIONS, WITH QUANTUM NUMBER ASSIGNMENTS, FOR THE ν_2 BAND OF $^{32}S^{16}O_2$ CENTERED AT 517.75±0.10 cm^{-1}. LINE INTENSITIES [SEE SEC. III, ESPECIALLY EQ. (6)] ARE COMPUTED AT 300°K. SEE SEC. III FOR Q SUB-BRANCH NOTATION.

Line Position (in cm^{-1})		Quantum Numbers						
Exptl.	Theor.	J'	K'_{-1}	K'_1	J"	K''_{-1}	K''_1	$\frac{I^{\circ}_{n''n'}}{C'}$
477.85	477.87	12	10	2	13	11	3	2.4590
	477.93	20	8	12	21	9	13	2.1097
478.56	478.51	11	10	2	12	11	1	2.5494
	478.58	19	8	12	20	9	11	2.2158
480.48	480.44	12	9	3	13	10	4	2.6890
	480.52	16	8	8	17	9	9	2.5200
480.85	480.86	29	5	25	30	6	24	1.3175
481.05	$Q_{\bar{1}1}$ (J, 13, K_1) sub-branch							
481.60	481.66	23	6	18	24	7	17	2.0091
482.68	482.65	56	0	56	57	1	57	0.3980
482.93	482.85	26	5	21	27	6	22	1.6756
	482.93	21	6	16	22	7	15	2.2448
483.38	$Q_{\bar{1}1}$ (J, 12, K_1) sub-branch							
484.16	484.21	19	6	14	20	7	13	2.4710
484.39	484.39	10	8	2	11	9	3	3.0456
484.90	484.86	18	6	12	19	7	13	2.5782
	484.93	27	4	24	28	5	23	1.4360
485.25	485.22	13	7	7	14	8	6	2.9402
	485.30	22	5	17	23	6	18	2.1642
485.67	485.68	8	8	0	9	9	1	3.2192
485.96	$Q_{\bar{1}1}$ (J, 11, K_1) sub-branch							
487.65	487.68	23	4	20	24	5	19	1.9687
	487.73	48	0	48	49	1	49	1.1589
488.04	488.07	13	6	8	14	7	7	3.0237
488.65	$Q_{\bar{1}1}$ (J, 10, K_1) sub-branch							
490.03	490.01	10	6	4	11	7	5	3.2090
	490.07	44	1	43	45	2	44	1.3835
490.32	490.25	19	4	16	20	5	15	2.4576
	490.39	14	5	9	15	6	10	2.9680
490.90	490.87	43	1	43	44	0	44	2.0315
	490.91	42	2	40	43	3	41	1.2273
	490.95	18	4	14	19	5	15	2.5685
491.30	$Q_{\bar{1}1}$ (J, 9, K_1) sub-branch							
492.02	492.04	40	2	38	41	3	39	1.4625
	492.12	41	1	41	42	0	42	2.4830
492.46	492.51	40	1	39	41	2	40	2.0497
492.70	492.74	40	0	40	41	1	41	2.7311
492.92	492.95	10	5	5	11	6	6	3.1747
493.13	493.06	19	3	17	20	4	16	2.1821
	493.12	38	2	36	39	3	37	1.7086
	493.15	39	2	38	40	1	39	2.2403
494.15	$Q_{\bar{1}1}$ (J, 8, K_1) sub-branch							
495.04	495.09	34	2	32	35	3	33	2.1816
495.24	495.23	36	0	36	37	1	37	3.8556
495.65	495.61	35	2	34	36	1	35	3.0684
495.95	495.85	35	1	35	36	0	36	4.1650
	495.93	32	2	30	33	3	31	2.3743
496.19	496.17	5	5	1	6	6	0	3.3267
497.14	$Q_{\bar{1}1}$ (J, 7, K_1) sub-branch							
498.28	498.25	24	2	22	25	3	23	2.6347
	498.31	31	1	31	32	0	32	5.4562
499.31	499.36	29	2	28	30	1	29	4.2949
499.98	$Q_{\bar{1}1}$ (J, 6, K_1) sub-branch							
500.62	500.64	26	1	25	27	2	26	4.7135
	500.66	27	2	26	28	1	27	4.6028
500.81	500.77	27	1	27	28	0	28	6.6981
	500.82	41	4	38	41	5	37	1.1296
501.67	501.64	24	1	23	25	2	24	4.8564
	501.72	12	2	10	13	3	11	2.5632
501.87	501.88	34	1	33	34	2	32	1.5773
502.08	501.99	25	1	25	26	0	26	7.2273
	502.08	38	5	33	38	6	32	1.5618
503.13	$Q_{\bar{1}1}$ (J, 5, K_1) sub-branch							
505.32	505.41	25	3	23	25	4	22	3.9681
505.48	505.44	32	4	28	32	5	27	2.9251
	505.52	5	2	4	6	3	3	2.2454
	505.56	14	1	13	15	2	14	3.6774
505.85	505.89	21	3	19	21	4	18	4.4600
506.20	$Q_{\bar{1}1}$ (J, 4, K_1) sub-branch							
506.53	506.48	16	3	13	16	4	12	4.4691
	506.53	19	2	18	20	1	19	4.4779
	506.57	23	2	22	23	3	21	3.7980
	506.60	7	1	7	8	2	6	1.4297
506.99	506.95	17	1	17	18	0	18	7.8932
	507.01	10	1	9	11	2	10	2.8783
507.17	507.21	16	0	16	17	1	17	7.7478
507.53	507.46	2	2	0	3	3	1	2.0263
	507.57	22	3	19	22	4	18	4.8466
508.26	$^{o}Q_{\bar{1}1}$ (J, 3, K_1) sub-branch							
508.45	508.45	21	3	19	22	2	20	2.2442
508.64	508.60	26	3	23	26	4	22	4.8183
	508.67	15	2	14	15	3	13	4.5439
509.30	$^{e}Q_{\bar{1}1}$ (J, 3, K_1) sub-branch							
510.03	509.97	12	2	10	12	3	9	4.5384
	510.03	28	2	26	28	3	25	4.8929
	510.06	25	4	22	26	3	23	1.3605
510.20	510.21	13	1	13	13	2	12	3.2827
510.52	510.52	22	1	21	22	2	20	5.2404
	510.54	19	3	17	20	2	18	2.0789
510.72	510.70	16	2	14	16	3	13	5.8705
510.89	510.89	11	1	11	11	2	10	3.2481
	510.96	11	1	11	12	0	12	6.0013
511.57	511.59	20	1	19	20	2	18	6.1756
511.75	511.77	13	2	12	14	1	13	2.9435

TABLE IV (Continued)

Line Position (in cm^{-1}) Exptl.	Theor.	Quantum Numbers J'	K'_{-1}	K'_1	J"	K''_{-1}	K''_1	$\frac{I^\circ_{n''n'}}{C'}$
512.28	512.23	6	0	6	7	1	7	3.6483
	512.24	14	0	14	14	1	13	4.1510
512.47	$^{o}Q_{\bar{1}1}$ (J, 2, K_1) sub-branch							
512.62	512.60	17	3	15	18	2	16	1.9041
513.30	$^{e}Q_{\bar{1}1}$ (J, 2, K_1) sub-branch							
513.53	513.46	10	1	9	10	2	8	5.7682
	513.49	12	1	11	12	2	10	6.8287
	513.57	11	2	10	12	1	11	2.3714
513.93	513.87	7	1	7	8	0	8	3.7376
	513.93	17	4	14	16	5	11	1.0946
514.13	514.12	22	5	17	21	6	16	1.0021
514.29	514.25	10	0	10	10	1	9	5.0873
	514.32	21	4	18	22	3	19	1.4202
514.52	514.47	13	3	11	12	4	8	1.0624
	514.58	15	3	13	16	2	14	1.7210
514.67	514.64	18	4	14	17	5	13	1.1410
514.90	514.94	8	0	8	8	1	7	5.1415
515.17	515.22	24	4	20	25	3	23	1.0300
	515.24	19	4	16	18	5	13	1.1729
515.48	515.44	6	0	6	6	1	5	4.6843
515.68	515.67	29	6	24	28	7	21	0.7352
	515.74	15	3	13	14	4	10	1.2221
516.03	516.02	20	4	16	19	5	15	1.1980
	516.04	22	4	18	23	3	21	1.1940
516.26	516.24	19	4	16	20	3	17	1.4281
517.24	517.19	13	2	12	12	3	9	1.2161
518.12	518.09	15	2	14	14	3	11	1.2397
	518.17	18	4	14	19	3	17	1.3614
518.27	518.23	11	3	9	12	2	10	1.3047
518.61	518.63	8	1	7	7	2	6	1.3067
518.75	518.72	4	0	4	3	1	3	1.4870
	518.75	12	3	9	13	2	12	1.2369
	518.80	17	2	16	16	3	13	1.1521
519.41	519.43	21	5	17	22	4	18	1.2345
520.05	520.09	6	1	5	6	0	6	4.7789
520.30	520.33	10	1	9	9	2	8	1.8594
520.53	520.58	8	1	7	8	0	8	5.2617
520.85	520.91	19	5	15	20	4	16	1.2371
521.10	521.11	13	4	10	14	3	11	1.1980
521.27	521.26	10	1	9	10	0	10	5.2304
521.68	521.71	18	5	13	19	4	16	1.2200
522.25	$^{e}Q_{1\bar{1}}$ (J, 1, K_1) sub-branch							
523.20	523.20	18	2	16	18	1	17	7.2577
523.37	$^{o}Q_{1\bar{1}}$ (J, 1, K_1) sub-branch							
524.12	524.18	9	2	8	9	1	9	3.2284
524.50	$^{e}Q_{1\bar{1}}$ (J, 2, K_1) sub-branch							
524.68	524.66	24	3	21	24	2	22	6.7275
	524.73	11	2	10	11	1	11	3.4597
525.00	525.07	26	3	23	26	2	24	6.0346
525.28	525.33	20	2	18	19	3	17	2.2149
525.76	525.77	28	3	25	28	2	26	5.1517
525.90	525.84	14	0	14	13	1	13	7.4305
526.32	526.32	24	2	22	24	1	23	4.6253
526.65	526.67	7	3	5	7	2	6	2.8812
	526.72	9	3	7	9	2	8	3.6547
526.95	$^{o}Q_{1\bar{1}}$ (J, 2, K_1) sub-branch							
527.71	527.72	26	2	24	26	1	25	3.8469
527.92	527.85	9	2	8	8	1	7	2.7471
	527.89	19	2	18	19	1	19	2.9963
	527.96	32	3	29	32	2	30	3.3811
528.16	528.13	17	1	17	16	0	16	8.5646
528.63	528.65	11	2	10	10	1	9	3.1947
	528.69	22	4	18	22	3	19	5.2661
528.90	528.90	13	6	8	14	5	9	0.7189
529.12	529.05	20	1	19	19	2	18	4.9613
529.25	$^{e}Q_{1\bar{1}}$ (J, 3, K_1) sub-branch							
529.65	529.59	18	4	14	18	3	15	5.1451
529.80	529.82	36	5	31	36	4	32	2.6035
530.07	530.07	14	4	10	14	3	11	4.6422
530.24	$^{o}Q_{1\bar{1}}$ (J, 3, K_1) sub-branch							
530.70	530.73	17	2	16	16	1	15	4.6239
	530.74	22	0	22	21	1	21	8.9777
530.90	530.86	42	4	38	42	3	39	1.3252
	530.92	36	3	33	36	2	34	2.0955
533.31	533.28	11	3	9	10	2	8	2.9320
	533.29	24	5	19	24	4	20	4.3585
533.64	533.63	27	1	27	26	0	26	8.1316
	533.64	30	1	29	30	0	30	1.4294
533.93	$Q_{1\bar{1}}$ (J, 4, K_1) sub-branch							
534.75	534.75	29	1	29	28	0	28	7.5521
	534.81	27	2	26	26	1	25	5.5536
535.01	535.02	15	3	13	14	2	12	3.0268
	535.06	39	5	35	39	4	36	1.6190
535.43	535.41	8	4	4	7	3	5	3.2619
536.00	536.00	30	1	29	29	2	28	5.1082
536.60	536.64	35	2	34	35	1	35	0.8993
537.20	537.16	23	3	21	22	2	20	3.1552
	537.20	32	1	31	31	2	30	4.7154
	537.26	5	5	1	4	4	0	3.6540
537.77	$Q_{1\bar{1}}$ (J, 5, K_1) sub-branch							
538.35	538.37	34	1	33	33	2	32	4.2627
538.65	538.63	36	0	36	35	1	35	5.1066
539.89	539.80	9	5	5	8	4	4	3.7478
	539.88	36	2	34	35	3	33	2.5561
540.74	540.75	17	4	14	16	3	13	3.2149
541.05	541.07	11	5	7	10	4	6	3.7836
541.65	$Q_{1\bar{1}}$ (J, 6, K_1) sub-branch							
542.60	542.54	21	4	18	20	3	17	2.8059
543.02	543.00	8	6	2	7	5	3	4.0887
543.28	543.21	23	4	20	22	3	19	2.5741
	543.25	20	4	16	19	3	17	2.7931
543.60	543.57	15	5	11	14	4	10	3.6865
	543.63	9	6	4	8	5	3	4.0833
544.24	544.20	16	5	11	15	4	12	3.6229
	544.26	10	6	4	9	5	5	4.0765
545.66	$Q_{1\bar{1}}$ (J, 7, K_1) sub-branch							
546.43	546.44	24	4	20	23	3	21	2.0716
546.91	546.89	8	7	1	7	6	2	4.3657
547.48	547.42	15	6	10	14	5	9	3.8951

TABLE IV (Continued)

Line Position (in cm^{-1})		Quantum Numbers						
Exptl.	Theor.	J'	K'_{-1}	K'_1	J"	K''_{-1}	K''_1	$\frac{I^{\circ}_{n''n'}}{C'}$
	547.52	9	7	3	8	6	2	4.3220
548.09	548.05	16	6	10	15	5	11	3.8209
	548.16	10	7	3	9	6	4	4.2826
549.47		Q_{11}^- (J, 8, K_1) sub-branch						
550.23	550.20	27	5	23	26	4	22	2.2072
550.64	550.69	14	7	7	13	6	8	4.0719
551.27	551.32	15	7	9	14	6	8	3.9951
551.52	551.48	9	8	2	8	7	1	4.4556
	551.52	31	5	27	30	4	26	1.6228
551.79	551.77	22	6	16	21	5	17	3.1327
	551.84	28	5	23	27	4	24	1.9979
552.01	551.95	16	7	9	15	6	10	3.9079
552.21	552.23	37	5	33	36	4	32	0.9895
552.40	552.37	23	6	18	22	5	17	2.9881
553.65		Q_{11}^- (J, 9, K_1) sub-branch						
554.66	554.65	14	8	6	13	7	7	4.0882
	554.73	27	6	22	26	5	21	2.3718
554.97	554.91	32	5	27	31	4	28	1.3379
555.25	555.29	15	8	8	14	7	7	3.9971
555.55	555.51	9	9	1	8	8	0	4.4820
555.93	555.92	16	8	8	15	7	9	3.8979
556.61	556.55	17	8	10	16	7	9	3.7900
	556.62	30	6	24	29	5	25	1.9049
556.98	556.94	24	7	17	23	6	18	2.8826
557.23	557.18	18	8	10	17	7	11	3.6733
557.85		Q_{11}^- (J, 10, K_1) sub-branch						
558.45	558.43	20	8	12	19	7	13	3.4175
558.66	558.68	14	9	5	13	8	6	4.0122
559.12	559.06	21	8	14	20	7	13	3.2799
	559.09	34	6	28	33	5	29	1.3324
559.37	559.31	15	9	7	14	8	6	3.9049
	559.38	28	7	21	27	6	22	2.2628
560.20	560.23	10	10	0	9	9	1	4.2829
560.43	560.40	36	6	30	35	5	31	1.0795
560.65	560.57	17	9	9	16	8	8	3.6857
	560.59	30	7	23	29	6	24	1.9594
560.87	560.86	11	10	2	10	9	1	4.1726
	560.93	24	8	16	23	7	17	2.8393
561.15	561.17	31	7	25	30	6	24	1.8125
561.60	561.55	25	8	18	24	7	17	2.6872
562.05		Q_{11}^- (J, 11, K_1) sub-branch						
563.13	563.09	21	9	13	20	8	12	3.1644
563.68	563.72	22	9	13	21	8	14	3.0219
564.25	564.35	23	9	15	22	8	14	2.8768
564.97	564.97	24	9	15	23	8	16	2.7291
	565.00	11	11	1	10	10	0	3.9697
565.25	565.23	31	8	24	30	7	23	1.7898
	565.29	18	10	8	17	9	9	3.3855
565.60	565.60	25	9	17	24	8	16	2.5807
	565.64	12	11	1	11	10	2	3.8531
565.84	565.84	32	8	24	31	7	25	1.6517
	565.87	19	10	10	18	9	9	3.2567
566.25		Q_{11}^- (J, 12, K_1) sub-branch						
567.15	567.19	21	10	12	20	9	11	2.9881
567.67	567.64	35	8	28	34	7	27	1.2692
567.82	567.81	22	10	12	21	9	13	2.8494
568.40	568.44	23	10	14	22	9	13	2.7087
568.88	568.81	17	11	7	16	10	6	3.2741
569.15	569.07	24	10	14	23	9	15	2.5665
569.44	569.44	18	11	7	17	10	8	3.1512
569.71	569.70	25	10	16	24	9	15	2.4242
570.09	570.07	19	11	9	18	10	8	3.0250
570.60		Q_{11}^- (J, 13, K_1) sub-branch						
571.06	571.11	14	12	2	13	11	3	3.3428
571.29	571.34	21	11	11	20	10	10	2.7653
571.52	571.57	28	10	18	27	9	19	2.0028
571.95	571.97	22	11	11	21	10	12	2.6327
572.40	572.38	16	12	4	15	11	5	3.1119
572.62	572.60	23	11	13	22	10	12	2.4991
573.08	573.01	17	12	6	16	11	5	2.9948
573.45	573.43	31	10	22	30	9	21	1.6058
573.70	573.65	18	12	6	17	11	7	2.8760
574.01	574.05	32	10	22	31	9	23	1.4819
574.48	574.48	26	11	15	25	10	16	2.0981
574.95		Q_{11}^- (J, 14, K_1) sub-branch						
575.25	575.28	34	10	24	33	9	25	1.2490
575.57	575.54	21	12	10	20	11	9	2.5098
576.55	576.51	36	10	26	35	9	27	1.0385
576.84	576.80	23	12	12	22	11	11	2.2611
577.23	577.27	17	13	5	16	12	4	2.6866
578.54	578.54	19	13	7	18	12	6	2.4617
579.15		Q_{11}^- (J, 15, K_1) sub-branch						
580.34	580.31	15	14	2	14	13	1	2.5724
	580.43	22	13	9	21	12	10	2.1207
581.05	581.07	23	13	11	22	12	10	2.0073
581.55	581.58	17	14	4	16	13	3	2.3647

sub-branches (corresponding to even- and odd-J transitions, resp., for $^{32}S^{16}O_2$) form two separate peaks in a Q sub-branch. As an example, the observed line positions in Table IV at 508.26 and 509.30 cm^{-1} correspond to the $^{o}Q_{\bar{1}1}(J,3,K_1)$ sub-branch and its even-J analog, resp. The left superscripts denote odd and even parity, resp., of the initial states; and the selection rules are explicitly $\Delta J = 0$, $\Delta K_{-1} = -1$ ($K_{-1} = 3 \rightarrow 2$ in this example), and $\Delta K_1 = +1$. In the particular cases of $Q_{\bar{1}1}(J,1,K_1)$ and $Q_{1\bar{1}}(J,0,K_1)$, both of which have only even sub-branches, it has been possible to resolve several individual transitions.

The observed positions of the Q sub-branches in the present work agree with those given previously by Shelton et al.[1] We have determined the band center of ν_2 to be at 517.75 ± 0.10 cm^{-1}. This value may be compared with the earlier results: 524 (Ref. 26), 517.84 (Ref. 27), 517.69 (Ref. 1), and 518.0 ± 0.5 cm^{-1} (Ref. 28).

The experimental and theoretical results for ν_3 in the spectral range from 1327.5 to 1390.0 cm^{-1} are represented in Fig. 3 and Table V. The selection rules,[25] different from those for ν_1 and ν_2, are $\Delta J = 0, \pm 1$; $J = 0 \nleftrightarrow J = 0$; but $\Delta K_{-1} = 0, \pm 2, \cdots$; and $\Delta K_1 = \pm 1, \pm 3, \cdots$. Because of the relatively large number of strong, closely spaced lines in ν_3,

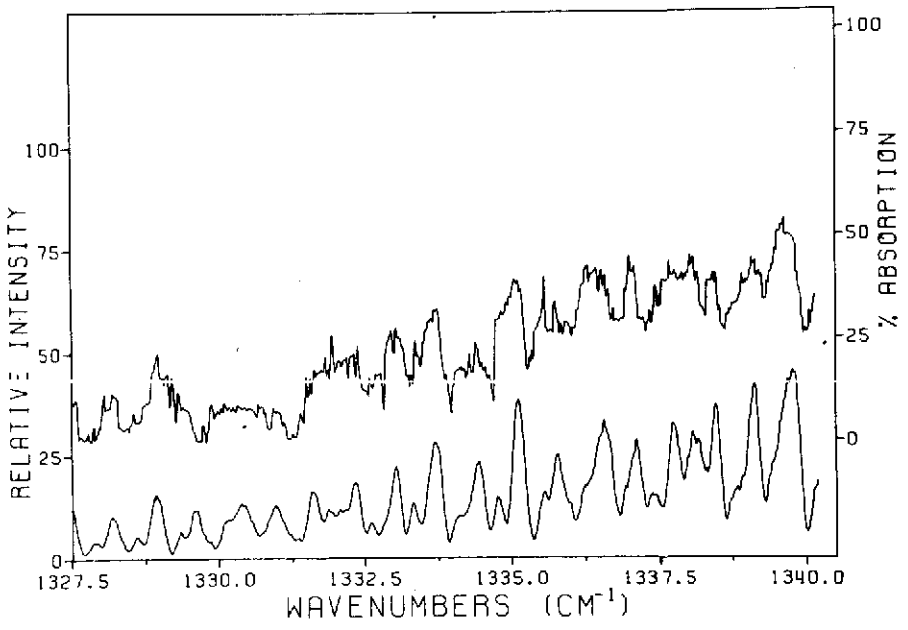

Fig. 3(a). Experimental and theoretical spectra of ν_3 band of $^{32}S^{16}O_2$ in range 1327.5 to 1340.0 cm^{-1}.

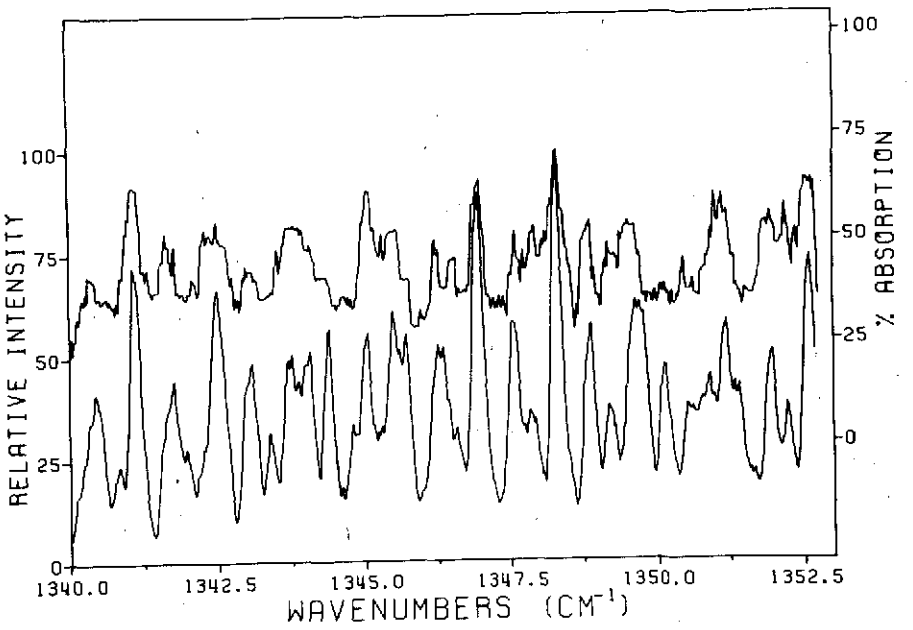

Fig. 3(b). Experimental and theoretical spectra of ν_3 band of $^{32}S^{16}O_2$ in range 1340.0 to 1352.5 cm^{-1}.

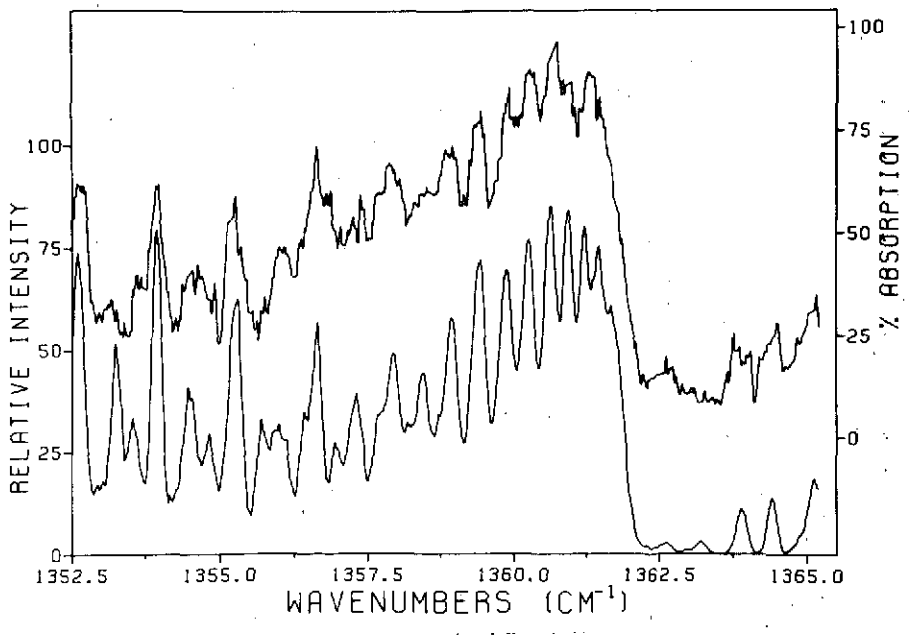

Fig. 3(c). Experimental and theoretical spectra of ν_3 band of $^{32}S^{16}O_2$ in range 1352.5 to 1365.0 cm^{-1}.

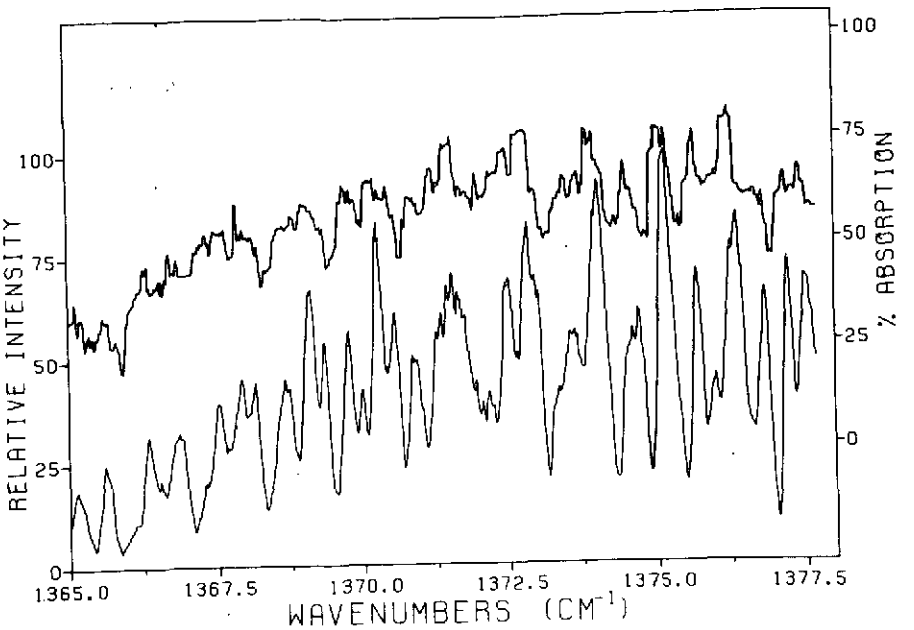

Fig. 3(d). Experimental and theoretical spectra of ν_3 band of $^{32}S^{16}O_2$ in range 1365.0 to 1377.5 cm^{-1}.

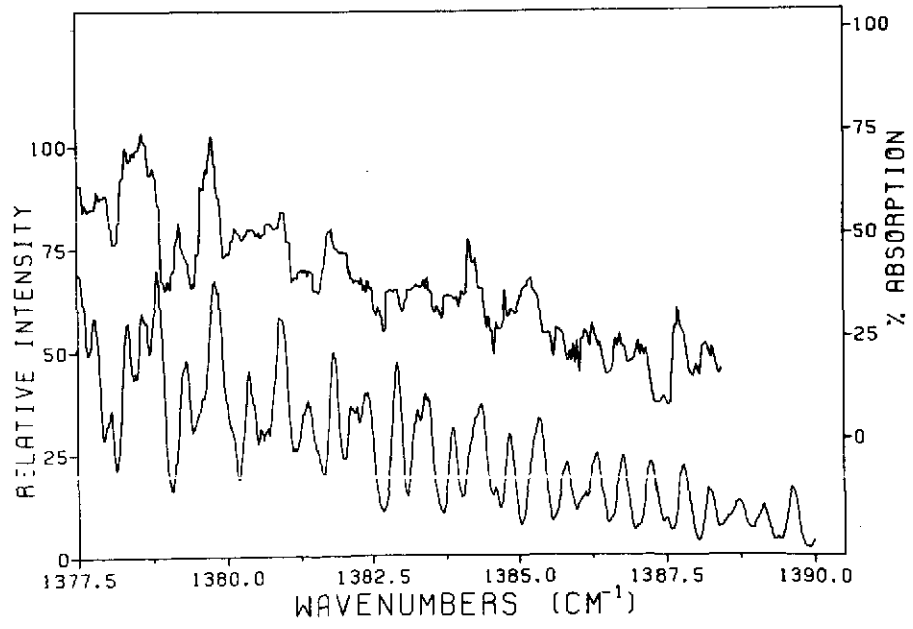

Fig. 3(e). Experimental and theoretical spectra of ν_3 band of $^{32}S^{16}O_2$ in range 1377.5 to 1390.0 cm^{-1}.

TABLE V

COMPARISON OF EXPERIMENTAL AND THEORETICAL SPECTRAL LINE POSITIONS, WITH QUANTUM NUMBER ASSIGNMENTS, FOR THE ν_3 BAND OF $^{32}S^{16}O_2$ CENTERED AT 1362.00±0.10 cm^{-1}. LINE INTENSITIES [SEE SEC. III, ESPECIALLY EQ. (6)] ARE COMPUTED AT 300°K.

Line Position (in cm^{-1})		Quantum Numbers							Line Position (in cm^{-1})		Quantum Numbers						
Exptl.	Theor.	J'	K'_{-1}	K'_1	J"	K''_{-1}	K''_1	$\frac{I^\circ_{n''n'}}{C'}$	Exptl.	Theor.	J'	K'_{-1}	K'_1	J"	K''_{-1}	K''_1	$\frac{I^\circ_{n''n'}}{C'}$
1327.57	1327.54	48	5	44	49	5	45	0.8793	1336.44	1336.43	38	2	37	39	2	38	3.6085
1327.73	1327.70	44	13	32	45	13	33	0.4210	1336.51	1336.52	35	7	28	36	7	29	2.9345
1327.87	1327.85	46	9	38	47	9	39	0.7091	1336.63	1336.63	33	11	22	34	11	23	1.7868
	1327.88	45	11	34	46	11	35	0.5683	1336.73	1336.73	30	15	16	31	15	17	0.8060
1328.05	1328.08	42	15	28	43	15	29	0.3207	1337.00	1336.99	34	8	27	35	8	28	2.7830
1328.16	1328.13	46	8	39	47	8	40	0.8186	1337.08	1337.10	37	1	36	38	1	37	3.9428
	1328.16	48	4	45	49	4	46	0.9741	1337.37	1337.35	32	11	22	33	11	23	1.9121
	1328.18	44	12	33	45	12	34	0.5234	1337.46	1337.46	34	6	29	35	6	30	3.5706
1328.55	1328.60	46	6	41	47	6	42	1.0321	1337.64	1337.65	34	5	30	35	5	31	3.9321
1328.97	1328.92	45	5	40	46	5	41	1.2401	1337.76	1337.75	32	10	23	33	10	24	2.3199
	1328.99	46	5	42	47	5	43	1.1368		1337.77	36	2	35	37	2	36	4.2919
	1329.01	45	6	39	46	6	40	1.1571	1338.02	1338.01	29	14	15	30	14	16	1.1119
1329.31	1329.35	45	4	41	46	4	42	1.3131	1338.08	1338.06	33	4	29	34	4	30	4.5280
1329.73	1329.75	43	10	33	44	10	34	0.8590	1338.17	1338.16	33	6	27	34	6	28	3.8584
1329.88	1329.86	44	7	38	45	7	39	1.1832		1338.19	33	5	28	34	5	29	4.2371
1330.08	1330.09	44	6	39	45	6	40	1.3180	1338.47	1338.47	34	3	32	35	3	33	4.6191
	1330.10	42	11	32	43	11	33	0.7988	1338.90	1338.91	32	6	27	33	6	28	4.1551
1330.65	1330.64	40	13	28	41	13	29	0.6436	1339.09	1339.09	32	5	28	33	5	29	4.5825
1330.93	1330.93	45	2	43	46	2	44	1.5717		1339.12	34	2	33	35	2	34	5.0326
	1330.97	44	4	41	45	4	42	1.5919	1339.63	1339.62	31	6	25	32	6	26	4.4531
1331.10	1331.12	42	8	35	43	8	36	1.3094	1340.12	1340.11	26	14	13	27	14	14	1.2229
1331.25	1331.23	41	10	31	42	10	32	1.0671		1340.13	30	7	24	31	7	25	4.2197
1331.37	1331.36	42	7	36	43	7	37	1.4874	1340.25	1340.25	29	9	20	30	9	21	3.3197
1331.49	1331.53	43	3	40	44	3	41	1.7931	1340.34	1340.33	31	2	29	32	2	30	5.7889
1331.61	1331.63	44	3	42	45	3	43	1.7629		1340.35	30	6	25	31	6	26	4.7537
1331.73	1331.71	46	1	46	47	1	47	1.7901	1341.35	1341.34	25	13	12	26	13	13	1.6383
1331.93	1331.96	40	10	31	41	10	32	1.1824	1341.64	1341.63	29	2	27	30	2	28	6.5907
1332.35	1332.37	42	4	39	43	4	40	1.9947		1341.66	27	9	18	28	9	19	3.6629
1332.56	1332.58	38	12	27	39	12	28	0.9705	1341.78	1341.77	30	2	29	31	2	30	6.6203
1333.02	1333.01	42	3	40	43	3	41	2.1971		1341.79	31	0	31	32	0	32	6.7894
	1333.03	43	1	42	44	1	43	2.2019	1342.29	1342.26	27	7	20	28	7	21	4.9739
	1333.05	40	6	35	41	6	36	2.0564		1342.28	25	11	14	26	11	15	2.6588
1333.34	1333.32	40	5	36	41	5	37	2.2595	1342.48	1342.45	30	1	30	31	1	31	7.2104
	1333.34	39	8	31	40	8	32	1.7895		1342.48	27	6	21	28	6	22	5.6251
1333.69	1333.67	41	2	39	42	2	40	2.4422		1342.51	27	3	24	28	3	25	7.1054
	1333.72	42	2	41	43	2	42	2.4470	1342.75	1342.73	23	13	10	24	13	11	1.6674
1334.13	1334.15	37	10	27	38	10	28	1.5709	1342.99	1342.96	26	7	20	27	7	21	5.2037
1334.29	1334.32	38	7	32	39	7	33	2.2456		1342.98	24	11	14	25	11	15	2.7207
1334.40	1334.39	40	3	38	41	3	39	2.7015	1343.51	1343.56	26	4	23	27	4	24	7.1252
	1334.40	41	1	40	42	1	41	2.7105	1344.05	1344.06	25	5	20	26	5	21	6.8310
1334.55	1334.53	38	6	33	39	6	34	2.5108		1344.07	25	4	21	26	4	22	7.4217
1334.83	1334.81	37	8	29	38	8	30	2.1613	1345.15	1345.15	22	9	14	23	9	15	4.2448
1335.05	1335.03	39	2	37	40	2	38	2.9837	1345.27	1345.23	24	3	22	25	3	23	8.3171
	1335.05	37	7	30	38	7	31	2.4647		1345.29	20	12	9	21	12	10	2.1121
	1335.08	37	4	33	38	4	34	3.1847		1345.30	23	6	17	24	6	18	6.5790
1335.56	1335.54	36	8	29	37	8	30	2.3610	1345.95	1345.97	19	12	7	20	12	8	2.0396
	1335.57	37	3	34	38	3	35	3.3480	1346.19	1346.16	21	8	13	22	8	14	5.1343
1335.74	1335.76	39	1	38	40	1	39	3.2917		1346.19	22	5	18	23	5	19	7.5469
1335.84	1335.80	40	1	40	41	1	41	3.3496	1346.26	1346.25	23	1	22	24	1	23	9.2116
1336.28	1336.26	35	8	27	36	8	28	2.5686	1346.60	1346.58	22	3	20	23	3	21	8.8762
	1336.32	34	10	25	35	10	26	2.0109	1346.99	1346.95	21	2	19	22	2	20	9.3946

TABLE V (Continued)

Line Position (in cm^{-1})		Quantum Numbers							Line Position (in cm^{-1})		Quantum Numbers						
Exptl.	Theor.	J'	K'_{-1}	K'_1	J"	K''_{-1}	K''_1	$\frac{I^\circ_{n''n'}}{C'}$	Exptl.	Theor.	J'	K'_{-1}	K'_1	J"	K''_{-1}	K''_1	$\frac{I^\circ_{n''n'}}{C'}$
	1346.97	23	0	23	24	0	24	9.8178	1354.50	1354.52	19	19	0	19	19	1	1.0675
	1347.01	22	2	21	23	2	22	9.4455		1354.53	10	4	7	11	4	8	6.7871
1347.18	1347.14	20	7	14	21	7	15	6.0759	1354.60	1354.55	9	7	2	10	7	3	2.8625
	1347.21	19	9	10	20	9	11	4.2616	1354.89	1354.92	8	8	1	9	8	2	0.9670
1347.30	1347.34	17	12	5	18	12	6	1.7973	1355.25	1355.24	19	18	1	19	18	2	1.2980
1347.38	1347.38	20	6	15	21	6	16	6.9817	1355.34	1355.30	9	1	8	10	1	9	8.1799
1347.49	1347.52	18	10	9	19	10	10	3.3407	1355.75	1355.73	23	17	6	23	17	7	0.9836
	1347.52	21	1	20	22	1	21	9.7377	1355.99	1355.99	8	3	6	9	3	7	6.4307
1347.59	1347.58	20	5	16	21	5	17	7.8440	1356.09	1356.12	8	2	7	9	2	8	7.1660
	1347.62	22	1	22	23	1	23	10.0823	1356.36	1356.34	7	5	2	8	5	3	3.5348
1347.72	1347.74	20	4	17	21	4	18	8.6200	1356.42	1356.42	8	1	8	9	1	9	7.6733
1347.91	1347.89	18	9	10	19	9	11	4.1884	1356.62	1356.61	18	16	3	18	16	2	2.0022
	1347.93	20	3	18	21	3	19	9.2815		1356.64	7	1	6	8	1	7	6.9194
1348.09	1348.07	19	6	13	20	6	14	7.0311		1356.64	7	3	4	8	3	5	5.6838
1348.31	1348.31	20	2	19	21	2	20	9.8640	1356.79	1356.78	6	6	1	7	6	2	1.2615
	1348.32	19	2	17	20	2	18	9.7829	1356.86	1356.87	25	15	10	25	15	11	1.0266
1348.86	1348.89	20	1	20	21	1	21	10.4854	1357.02	1357.00	6	5	2	7	5	3	2.5490
1348.95	1348.96	18	5	14	19	5	15	7.9514	1357.23	1357.22	18	15	4	18	15	3	2.2695
1349.15	1349.12	18	4	15	19	4	16	8.7841		1357.26	17	15	2	17	15	3	2.5354
	1349.14	15	11	4	16	11	5	2.0407	1357.35	1357.33	15	15	0	15	15	1	3.1678
1349.35	1349.36	14	12	3	15	12	4	1.1363	1358.05	1358.03	5	2	3	6	2	4	4.8131
1349.50	1349.51	19	0	19	20	0	20	10.6170	1358.20	1358.18	5	0	5	6	0	6	5.5900
1349.69	1349.71	17	2	15	18	2	16	9.9530		1358.22	20	13	8	20	13	7	2.1608
1349.81	1349.78	17	3	14	18	3	15	9.4805	1358.29	1358.27	19	13	6	19	13	7	2.4155
	1349.81	14	11	4	15	11	5	1.7620		1358.31	18	13	6	18	13	5	2.6989
1349.94	1349.92	15	9	6	16	9	7	3.6733	1358.50	1358.49	13	13	0	13	13	1	4.7290
1350.05	1350.06	17	1	16	18	1	17	10.2536	1358.83	1358.84	17	12	5	17	12	6	3.1241
1350.15	1350.12	16	6	11	17	6	12	6.8587		1358.85	26	11	16	26	11	15	1.1498
	1350.16	18	1	18	19	1	19	10.6817	1358.94	1358.95	14	12	3	14	12	2	4.4117
1350.26	1350.23	14	10	5	15	10	6	2.5161	1359.12	1359.12	21	11	10	21	11	11	2.0498
	1350.26	15	8	7	16	8	8	4.6333	1359.23	1359.21	19	11	8	19	11	9	2.5636
1350.36	1350.33	16	5	12	17	5	13	7.8310	1359.43	1359.40	14	11	4	14	11	3	4.4770
1350.48	1350.49	16	4	13	17	4	14	8.7144		1359.43	13	11	2	13	11	3	5.0204
1350.63	1350.60	14	9	6	15	9	7	3.3877	1359.92	1359.90	11	10	1	11	10	2	6.2507
	1350.64	16	3	14	17	3	15	9.4630		1359.92	10	10	1	10	10	0	7.0834
1351.00	1351.00	15	5	10	16	5	11	7.6742		1359.95	20	9	12	20	9	11	2.1295
1351.11	1351.11	15	2	13	16	2	14	9.8638	1360.04	1360.03	18	9	10	18	9	9	2.6611
1351.21	1351.20	15	3	12	16	3	13	9.3354	1360.27	1360.27	11	9	2	11	9	3	5.9171
	1351.22	14	7	8	15	7	9	5.3836		1360.29	10	9	2	10	9	1	6.7055
1351.94	1351.94	12	9	4	13	9	5	2.6131	1360.35	1360.36	18	8	11	18	8	10	2.4157
1352.19	1352.15	13	6	7	14	6	8	6.1112	1360.84	1360.84	13	7	6	13	7	7	3.6683
	1352.22	14	2	13	15	2	14	9.7916	1361.06	1361.06	14	6	9	14	6	8	2.6706
1352.37	1352.35	13	5	8	14	5	9	7.1475	1361.45	1361.45	7	5	2	7	5	3	5.0069
1352.53	1352.51	13	2	11	14	2	12	9.4830		1361.46	6	5	2	6	5	1	5.8958
	1352.56	12	7	6	13	7	7	4.6334	1362.20	1362.18	9	2	7	9	2	8	0.6800
1352.63	1352.60	13	3	10	14	3	11	8.9012	1362.64	1362.64	1	0	1	0	0	0	0.9982
	1352.65	13	1	12	14	1	13	9.8033	1363.89	1363.89	3	0	3	2	0	2	2.9686
1352.96	1352.94	11	8	3	12	8	4	3.0805	1363.99	1363.96	3	1	2	2	1	1	2.6174
1353.17	1353.19	12	4	9	13	4	10	7.7426	1364.49	1364.45	4	2	3	3	2	2	2.8490
1353.25	1353.23	13	0	13	14	0	14	10.1011	1364.83	1364.85	5	4	1	4	4	0	1.5310
	1353.27	10	9	2	11	9	3	1.5169	1365.15	1365.13	5	0	5	4	0	4	4.8434
1353.59	1353.60	10	8	3	11	8	4	2.4852	1365.24	1365.26	5	1	4	4	1	3	4.6113
1353.68	1353.69	11	5	6	12	5	7	6.3101	1365.60	1365.60	6	1	6	5	1	5	5.5369
1353.91	1353.89	10	7	4	11	7	5	3.5504	1365.69	1365.70	6	2	5	5	2	4	4.9313
	1353.91	11	2	9	12	2	10	8.7906	1366.27	1366.24	7	3	4	6	3	3	4.9816
	1353.93	12	1	12	13	1	13	9.7348	1366.36	1366.34	7	0	7	6	0	6	6.5562
1353.98	1353.97	11	1	10	12	1	11	9.1436	1366.56	1366.54	7	1	6	6	1	5	6.3656
1354.23	1354.26	9	8	1	10	8	2	1.7865	1366.72	1366.69	9	7	2	8	7	1	2.1342
1354.35	1354.36	10	5	6	11	5	7	5.7641		1366.72	8	4	5	7	4	4	4.8364

TABLE V (Continued)

Line Position (in cm^{-1})		Quantum Numbers							Line Position (in cm^{-1})		Quantum Numbers						
Exptl.	Theor.	J'	K'_{-1}	K'_1	J"	K''_{-1}	K''_1	$\frac{I^\circ_{n''n'}}{C'}$	Exptl.	Theor.	J'	K'_{-1}	K'_1	J"	K''_{-1}	K''_1	$\frac{I^\circ_{n''n'}}{C'}$
1366.87	1366.86	8	3	6	7	3	5	5.8689		1376.25	24	5	20	23	5	19	8.0821
1367.36	1367.34	9	4	5	8	4	4	5.6831	1376.81	1376.82	25	1	24	24	1	23	9.8080
1367.64	1367.67	9	2	7	8	2	6	7.4212	1377.19	1377.18	26	6	21	25	6	20	6.8219
1367.85	1367.81	9	1	8	8	1	7	7.8726		1377.20	25	4	21	24	4	20	8.5470
1367.95	1367.94	10	1	10	9	1	9	8.6178		1377.22	26	2	25	25	2	24	9.4444
	1367.96	10	4	7	9	4	6	6.4331	1377.42	1377.42	28	9	20	27	9	19	4.0979
1368.12	1368.15	10	2	9	9	2	8	8.1114		1377.43	26	5	22	25	5	21	7.5853
1368.21	1368.24	12	8	5	11	8	4	3.2321	1377.63	1377.61	25	3	22	24	3	21	9.0766
1368.65	1368.65	11	0	11	10	0	10	9.3010	1377.83	1377.84	27	1	26	26	1	25	9.1025
1368.81	1368.79	12	6	7	11	6	6	5.4902	1378.31	1378.31	29	0	29	28	0	28	8.9600
	1368.85	13	8	5	12	8	4	3.7762		1378.34	29	8	21	28	8	20	4.6134
1369.29	1369.33	12	3	10	11	3	9	8.5616	1378.44	1378.46	27	4	23	26	4	22	7.9100
1369.37	1369.35	12	2	11	11	2	10	9.2530	1378.60	1378.57	30	9	22	29	9	21	3.7439
	1369.40	13	6	7	12	6	6	6.0186		1378.61	28	5	24	27	5	23	6.9791
1369.73	1369.73	15	9	6	14	9	5	3.5974	1378.79	1378.76	28	4	25	27	4	24	7.5913
	1369.76	13	0	13	12	0	12	10.2737	1379.03	1379.03	33	12	21	32	12	20	1.7647
1369.84	1369.80	13	4	9	12	4	8	8.1565	1379.20	1379.23	30	7	24	29	7	23	5.0511
	1369.82	18	13	6	17	13	5	1.3549	1379.58	1379.58	29	2	27	28	2	26	7.8515
1370.00	1369.99	13	3	10	12	3	9	9.0279	1379.66	1379.66	35	13	22	34	13	21	1.2346
	1370.01	14	6	9	13	6	8	6.4635	1379.77	1379.73	30	3	28	29	3	27	7.3461
1370.22	1370.22	14	1	14	13	1	13	10.6174		1379.78	30	5	26	29	5	25	6.3026
	1370.26	13	1	12	12	1	11	10.0292		1379.81	31	7	24	30	7	23	4.7786
1370.31	1370.31	18	12	7	17	12	6	1.9317	1380.01	1380.01	29	3	26	28	3	25	7.5615
	1370.33	16	9	8	15	9	7	3.9163	1380.14	1380.12	31	6	25	30	6	24	5.3833
1370.43	1370.41	14	4	11	13	4	10	8.5657	1380.37	1380.35	32	2	31	31	2	30	7.0310
1370.57	1370.55	14	3	12	13	3	11	9.4218		1380.37	33	0	33	32	0	32	7.2039
1370.70	1370.67	16	8	9	15	8	8	4.9398	1380.55	1380.57	31	2	29	30	2	28	6.9989
1370.88	1370.85	15	0	15	14	0	14	10.9608	1381.16	1381.15	31	3	28	30	3	27	6.7141
	1370.90	19	12	7	18	12	6	2.0889	1381.33	1381.36	34	2	33	33	2	32	6.1753
1370.98	1370.96	16	7	10	15	7	9	6.0231	1381.82	1381.83	34	3	32	33	3	31	5.7009
1371.31	1371.34	16	1	16	15	1	15	11.1751	1382.31	1382.34	36	8	29	35	8	28	2.9679
1371.44	1371.44	15	1	14	14	1	13	10.6475	1382.42	1382.40	37	0	37	36	0	36	5.4550
	1371.44	16	5	12	15	5	11	8.1824	1382.58	1382.54	37	9	28	36	9	27	2.3546
1371.55	1371.54	15	2	13	14	2	12	10.3274	1383.36	1383.39	39	0	39	38	0	38	4.6460
1371.68	1371.67	22	14	9	21	14	8	1.3021	1383.44	1383.44	35	4	31	34	4	30	4.8160
	1371.69	16	2	15	15	2	14	10.6161	1383.60	1383.63	37	6	31	36	6	30	3.4994
1371.98	1371.94	17	0	17	16	0	16	11.3605	1383.94	1383.94	41	11	30	40	11	29	1.1589
	1371.95	20	11	10	19	11	9	2.9085	1384.03	1384.03	39	8	31	38	8	30	2.3047
1372.18	1372.16	18	7	12	17	7	11	6.4341	1384.14	1384.13	38	6	33	37	6	32	3.2140
1372.47	1372.44	18	1	18	17	1	17	11.4436		1384.17	37	5	32	36	5	31	3.8266
	1372.47	19	8	11	18	8	10	5.5112	1384.24	1384.22	38	4	35	37	4	34	3.8372
1372.78	1372.76	19	7	12	18	7	11	6.5472		1384.25	37	3	34	36	3	33	4.2622
1372.97	1372.96	18	3	16	17	3	15	10.2187	1384.49	1384.49	42	11	32	41	11	31	1.0509
1373.28	1373.26	19	5	14	18	5	13	8.5806	1384.61	1384.59	40	8	33	39	8	32	2.1014
1373.70	1373.68	19	1	18	18	1	17	11.0036		1384.61	37	4	33	36	4	32	4.0726
1373.85	1373.86	20	5	16	19	5	15	8.5855	1384.78	1384.77	41	9	32	40	9	31	1.6462
1373.96	1373.96	20	2	19	19	2	18	10.8171		1384.81	39	6	33	38	6	32	2.9327
1374.34	1374.30	24	11	14	23	11	13	3.0426	1385.86	1385.85	44	1	44	43	1	43	2.9281
1374.49	1374.46	21	5	16	20	5	15	8.5330	1385.99	1386.00	41	6	35	40	6	34	2.4187
1375.17	1375.14	23	7	16	22	7	15	6.4815	1386.27	1386.25	42	4	39	41	4	38	2.6238
	1375.16	23	0	23	22	0	22	10.9944		1386.30	44	2	43	43	2	42	2.6030
1375.42	1375.41	23	6	17	22	6	16	7.4030	1386.38	1386.37	42	6	37	41	6	36	2.1911
	1375.43	24	8	17	23	8	16	5.4631	1386.64	1386.65	41	5	36	40	5	35	2.6254
1375.66	1375.66	23	5	18	22	5	17	8.2759	1386.74	1386.78	45	1	44	44	1	43	2.3430
	1375.68	24	1	24	23	1	23	10.7412	1387.02	1387.03	43	3	40	42	3	39	2.3802
1376.03	1376.00	24	6	19	23	6	18	7.2437	1387.70	1387.73	47	1	46	46	1	45	1.8796
1376.14	1376.15	24	2	23	23	2	22	10.0732	1388.03	1388.06	47	9	38	46	9	37	0.8565
	1376.17	28	12	17	27	12	16	2.2261	1388.17	1388.20	46	4	43	45	4	42	1.6966
1376.24	1376.22	25	0	25	24	0	24	10.4499	1388.29	1388.29	46	7	40	45	7	39	1.2628

we have assigned only the approximately 250 observed peaks which are either individual or consist of a small number of closely spaced transitions. The band center for ν_3 in the present work has been determined as 1362.00 ± 0.10 cm^{-1}. Previously obtained values were 1361 (Ref. 26), 1361.50 (Ref. 27), 1361.76 (Ref. 1), 1360.5 ± 0.5 (Ref. 28), and 1360.8 cm^{-1} (Ref. 29).

Finally, we have estimated the absolute values of the dipole moment derivatives[31] for all three infrared-active fundamentals of $^{32}S^{16}O_2$. Our analysis, using Eqs.(6) and (7), was described in detail in Sec. III. The results are shown in Table VI. The ν_1 band intensity of Hinkley et al.[8] was an average of the projected values which were obtained by dividing the intensities of ten measured lines by their respective calculated fractional contributions to the band.

TABLE VI

DIPOLE MOMENT DERIVATIVES FOR THE FUNDAMENTALS OF $^{32}S^{16}O_2$

Band	Sum of Calculated Line Intensities (dimensionless)	Measured Band Intensity (in $10^{10} sec^{-1} cm^{-1}$ STP)	Dipole Moment Derivative[f] (in esu $g^{-1/2}$)
ν_1	5227.9	278 ± 28[a]	57.8 ± 3.0
		317 ± 8[b]	61.7 ± 0.8
		350 ± 20[c]	64.8 ± 1.9
		288 ± 16[d]	58.9 ± 1.7
		299 ± 16[e]	59.9 ± 1.6
ν_2	5288.6	348 ± 35[a]	64.3 ± 3.3
		376 ± 20[b]	66.8 ± 1.8
		360 ± 30[c]	65.4 ± 2.8
ν_3	5742.3	2520 ± 252[a]	166.0 ± 9.0
		2560 ± 70[b]	167.3 ± 2.3
		2640 ± 80[c]	169.9 ± 2.6
		2437 ± 161[e]	163.1 ± 5.5

[a]From Ref. 20.
[b]From Ref. 21.
[c]From Ref. 22.
[d]From Ref. 8.
[e]From Ref. 23.
[f]As discussed in Sec. III, only the absolute value can be determined here.

V. DISCUSSION

There is considerable value, from a fundamental spectroscopic viewpoint, in making high-resolution studies of gases like SO_2. Such studies would permit a more complete determination of vibration-rotation line positions and intensities, as well as quantum-number assignments, in all three fundamentals. Further, it would be possible to measure line-shapes and line-broadening parameters as a function of vibration and/or rotation quantum numbers. Some of these experimental and theoretical studies are in progress, and some are anticipated in our laboratory in the near future.

We also plan to investigate overtone and combination bands of SO_2. A more precise determination of the band center of $2\nu_2$ is important to an understanding of possible lasing mechanisms[32] in SO_2, associated with Fermi interactions between energy levels in ν_1 and $2\nu_2$. In another context, it is possible that the $\nu_1 + \nu_3$ band of terrestrial SO_2 may appear in solar spectra,[33] and be susceptible to analysis there.

Sulfur dioxide plays a serious role as a pollutant in the terrestrial atmosphere.[34] High-resolution infrared spectroscopy is a possible technique for the remote detection and monitoring of SO_2 in situ. For example, monochromatic laser emissions may be useful for studying terrestrial SO_2 in absorption. We have found three relatively isolated and moderately strong lines in our laboratory spectra, with observed positions at 561.67, 1347.33, and 1365.60 cm^{-1} (see Tables IV and V) which fall close to observed laser oscillations[35] in pure neutral neon, Ne I. Although the spectral coincidences are not exact for the first two lines, nevertheless the spectral broadening by air will produce sufficient overlapping of the lines in question.[36]

ACKNOWLEDGMENTS

We are grateful to Prof. W. H. Fletcher for several helpful discussions, and for a critical reading of this manuscript. Prof. D. F. Eggers, Jr. provided a computer program, developed by Dr. L. Pierce and modified by Prof. Eggers, which was of considerable value in our calculations. Dr. E. D. Hinkley kindly sent us preprints of Refs. 8 and 9. We thank Mr. Glen H. Cunningham of our Electronics Shop for his generous and skillful technical assistance. Mrs. Janice Hemsley typed the manuscript with accuracy and patience. We appreciate the time provided by The University of Tennessee Computing Center on the IBM/360-65 system.

REFERENCES

1. R. D. Shelton, A. H. Nielsen, and W. H. Fletcher, J. Chem. Phys. 21, 2178 (1953). References to earlier microwave and infrared measurements are given in this work.
2. Y. Morino, Y. Kikuchi, S. Saito, and E. Hiroto, J. Mol. Spectry. 13, 95 (1964).
3. R. Van Riet, Ann. Soc. Sci. Bruxelles 78, 237 (1964).
4. H. A. Gebbie, N. W. B. Stone, G. Topping, E. K. Gora, S. A. Clough, and F. X. Kneizys, J. Mol. Spectry. 19, 7 (1966).
5. G. Steenbeckeliers, Ann. Soc. Sci. Bruxelles 82, 331 (1968).
6. S. Saito, J. Mol. Spectry. 30, 1 (1969).
7. Additional references, including work on various isotopic forms, are given by A. Barbe and P. Jouve, J. Mol. Spectry. 38, 273 (1971).
8. E. D. Hinkley, A. R. Calawa, P. L. Kelley, and S. A. Clough, J. Appl. Phys. 43, 3222 (1972).
9. P. L. Kelley and E. D. Hinkley, in Fundamental and Applied Laser Physics, edited by M. S. Feld, N. Kurmit, and A. Javan (John Wiley and Sons, New York, 1972).
10. IUPAC, Tables of Wavenumbers for the Calibration of Infrared Spectrometers (Butterworth, London, 1961).
11. J. Overend and R. W. Thompson, Proc. Roy. Soc. (London) A232, 291 (1955).
12. G. Herzberg, Infrared and Raman Spectra of Polyatomic Molecules (Van Nostrand, Princeton, N. J., 1945).
13. H. C. Allen, Jr. and P. C. Cross, Molecular Vib-Rotors (John Wiley and Sons, New York, 1963).
14. D. Kivelson and E. Bright Wilson, Jr., J. Chem. Phys. 20, 1575 (1952).
15. L. Pierce, N. Di Cianni, and R. H. Jackson, J. Chem. Phys. 38, 730 (1963).
16. See, for example, S. S. Penner, Quantitative Molecular Spectroscopy and Gas Emissivities (Addison-Wesley, Reading, Mass.,1959), p. 158.
17. M. T. Emerson and D. F. Eggers, Jr., J. Chem. Phys. 37, 251 (1962).
18. D. F. Eggers, Jr., private communication, 1971.
19. K. G. Kidd and G. W. King, J. Mol. Spectry. 40, 461 (1971).
20. D. F. Eggers, Jr. and E. D. Schmid, J. Phys. Chem. 64, 279 (1960).
21. J. E. Mayhood, Can. J. Phys. 35, 954 (1957).
22. J. Morcillo and J. Herranz, Publs. Inst. Quim. Fis. "Rocasolano" 10, 162 (1956).
23. D. E. Burch, J. D. Pembrook, and D. A. Gryvnak, Philco-Ford Publ. No. U-4947, July, 1971.
24. R. J. Corice, Jr., K. Fox, and G. D. T. Tejwani, J. Chem. Phys., to be published January, 1973.

25. P. C. Cross, R. M. Hainer, and G. W. King, J. Chem. Phys. 12, 210 (1944).

26. C. R. Bailey and A. B. D. Cassie, Proc. Roy. Soc. (London) A140, 605 (1933).

27. E. F. Barker, Rev. Mod. Phys. 14, 198 (1942).

28. S. R. Polo and M. K. Wilson, J. Chem. Phys. 22, 900 (1954).

29. E. C M. Grigg and G. R. Johnston, Australian J. Chem. 19, 1147 (1966).

30. E. D. Hinkley, MIT-Lincoln Lab. Rept., March 31, 1972.

31. G. D. T. Tejwani, K. Fox, and R. J. Corice, Jr., to be published.

32. G. Hubner, J. C. Hassler, P. D. Coleman, and G. Steenbeckeliers, Appl. Phys. Letters 18, 511 (1971).

33. D. N. B. Hall, private communication, 1972.

34. W. W. Kellog, R. D. Cadle, E. R. Allen, A. L. Lazrus, and E. A. Martell, Science 175, 587 (1972). An extensive bibliography on sulfur compounds in the atmosphere and oceans is given in this review article.

35. W. S. C. Chang, Principles of Quantum Electronics (Addison-Wesley, Reading, Mass., 1969).

36. G. D. T. Tejwani, J. Chem. Phys., to be published December, 1972.